Microfluid Nanofluid (2011) 10:703–734
DOI 10.1007/s10404-010-0716-y

REVIEW

Microfluidics cell electroporation

Saeid Movahed · Dongqing Li

Received: 10 August 2010 / Accepted: 4 October 2010 / Published online: 19 October 2010

Abstract Electroporation or electropermeabilization is one of the most powerful biological techniques in cell studies. Applying the high voltage electric field in vicinity of the cells can generate nanopores in cell membrane. Varying with the intensity and the duration of these applied electric field, the created nanopores can be temporary (reversible electroporation) or permanent (irreversible electroporation). Reversible electroporation is usually conducted to insert biological samples into the cells. Cells are also electroporated irreversibly to release their intercellular contents for further biological investigations. In comparison with the conventional electroporation devices, microfluidic (microscale) electroporation devices have some advantages such as higher cell viability rate, high transfection efficiency, lower sample contamination, and smaller Joule heating effect. In this article, the latest advancement in microfluidic cell electroporation is reviewed. First, the underlying theory of membrane permeabilization is reviewed and the leading analytical studies on the cell electroporation are presented. Following that, different experimental methods are compared. Finally, some suggestions are proposed for the future studies.

Keywords Electroporation · Cell · Microfluidics · Lab-on-a-chip

S. Movahed · D. Li (✉)
Department of Mechanical and Mechatronics Engineering, University of Waterloo, Waterloo, ON N2L 3G1, Canada
e-mail: dongqing@mme.uwaterloo.ca

1 Introduction

Electric field is widely applied in microfluidics for various applications, e.g., generating liquid motion by electroosmosis, and separating molecules by electrophoresis (Li 2004, 2008a). Non-uniform electric fields can generate motion of dielectric particles without electrostatic charge, which is referred to as the dielectrophoresis. Dielectrophoresis can be utilized to separate cells by size (Kang et al. 2008) or control the orientation of the cells (Valley et al. 2009b). The other important effects of applied electric field in microfluidic devices include Joule heating. Excessive Joule heating can be harmful for biological cells and must be prevented.

One of the most interesting influences of applied electric field on cells is electroporation. Applying electric field near the cell results in disturbance in cell membrane structure and creating nanopores in cell membrane. This leads to a significant increase in the electrical conductivity and permeability of the cell membrane that is usually refers as a *electroporation* or *electropermeabilization* (Weaver and Chizmadzhev 1996; Teissie et al. 2005; Li 2008b; Escoffre et al. 2009; Neu and Neu 2009).

Because of the difference between intracellular and extracellular conductivities, the ability of the cell membrane to act as a capacitance, and the existence of the electric current in the cell membrane due to ion pumps and ion channels, there is a discontinuity between the electric potential on the two sides of the cell membrane (DeBruin and Krassowska 1999a). This difference is called the transmembrane potential (TMP). At each point of the cell membrane, the TMP is linearly proportional to the external electric field and the cell diameter. For spherical cells, the TMP can be calculated by the following equation (DeBruin and Krassowska 1999a, b):

$$\mathrm{TMP} = \phi_i - \phi_o = 1.5 r_{\mathrm{cell}} E_{\mathrm{e}} \cos(\theta) \quad (1)$$

where r_{cell} is the radius of the cell, E_{e} is the external electric field, and θ is the angle between the site on the cell membrane where TMP is measured and the direction of E_{e}.

The TMP can affect the membrane structure and cause nanopores. These pores are initially hydrophobic; at the TMP threshold value of 0.5–1.0 V the pores turns into hydrophilic (Neu and Neu 2009) (the governing theory of this pore generation will be explained later in this review). Depending on the duration and the intensity of the applied electric pulse, the created pores may be transient or permanent. For low and short-duration electric fields, the pores can reseal themselves when the applied electrical field is removed. However, strong-intensity and long-duration electric fields can cause irreversible distortions and permanent nanopores in cell membrane. The generated reversible or irreversible nanopores may be used for different applications such as cell lysis, transfection pasteurization, and electrofusion.

Traditional electroporation devices suffer from a number of problems: in addition to the insufficient understanding of its theoretical mechanism, the cell viability and electroporation efficiency are inadequate; some cells are distorted while others are unaffected. The cell viability is typically about 20–50% and transfection rate for mammalian cell lines is less than 50% (Lee et al. 2009). Because of the large size of these devices, excessive voltage must apply to the electrodes in order to generate the required electric field for electroporation. Special safety cautions are required to operate commercial electroporators at several hundred volts. The large distances between the electrodes in conjunction with the short-duration electric pulses can also lead to a non-uniform and less stable electric field profile. Furthermore, the conventional electroporators usually have sensitive and complicated experimental processes. Aluminum-based electrodes are widely used in commercial instruments that could be a source of Al^{3+} ions dissolved into the media, leading to unpredictable results in cells (Kim et al. 2007).

On the contrary, microfluidic electroporation can provide spatial and temporal control of various electrical parameters. Many shortcomings of convectional electroporation such as variations in the local pH, electric field distortion, sample contamination, and the difficulties in transfection and maintaining the viability of desired cell types can be avoided in microfluidic electroporation. This review article is focused on the recent advances of microfluidic-based cell electroporation.

They are many advantages associate with the microfluidic electroporation (Fox et al. 2006; Lee et al. 2009). The required voltages in the microfluidic devices are much lower in comparison with the macroscopic systems. By shrinking the inter-electrode distance to a few tens of microns, it is possible to reduce the voltage requirement to a few volts (three orders of magnitude smaller than typical voltages required in a macroscopic apparatus). Consequently, the power consumption (P) becomes six orders of magnitude smaller ($P \propto V^2$) and heat generation is minimal. One of the challenging problems of conventional electroporation systems is the heat generation. In microscale devices, the area-to-volume ratio is relatively large. This leads to the faster heat dissipation. The fast dissipation of the generated heat makes it possible to distinguish the heating effects and the electric field effects. The ability of performing electroporation process in continuous flow is another advantage of microfluidic electroporation devices. The required amounts of difficult-to-produce reagents, such as specific plasmids, are considerably small in comparison with conventional electroporation. Microfluidic electroporation has the ability of in situ visualization of molecular uptake. One can have a real-time monitoring of intracellular response to the external electric pulses (using fluorescent probes for example). The ability to perform the single cell electroporation is a further advantage of the microfluidic electroporation. In microfluidic electroporation, it is possible to trap single cells and perform transfection or determine intracellular content or other properties of a single cell, which is hardly feasible when using conventional equipment. One can have more symmetrical and uniform electric fields in microfluidic electroporative devices. Cell handling and manipulation are also easier in microfluidic electroporation. Last but not the least is the potential of microfluidics electroporative devices for integration with other microfluidic components to form a multifunction a lab-on-chip system for subcellular analysis, which would greatly facilitate large-scale biochemical experimentations.

Especially in the previous decade, theoretical studies on cell electroporation have lagged behind the experimental ones. Due to the recent progress on microfabrication techniques (Ziaie et al. 2004), many researchers concentrated on the design and fabrication of the microscale electroporative devices. Although some theoretical studies have been conducted on cell electroporation (Weaver and Chizmadzhev 1996; Teissie et al. 2005; Li 2008b; Escoffre et al. 2009; Neu and Neu 2009; Escoffre et al. 2009), there are many ambiguities associated with cell electroporation, e.g., there is no definite hypothesis about the exact mechanism of cell transfection.

In the past decade, some review articles have been published on the experimental studies of cell electroporation. Fox et al. reviewed the experimental studies of the electroporation of cells in microfluidic devices prior to 2006. According to this review article, the electroporation microdevices have three main applications: analyzing

cellular properties or intracellular content, transfecting cells, and inactivating/pasteurizing cells. Another review article was published in 2009 (Lee et al. 2009). This review article divided the microfluidic electroporative devices into two categories: microchannels-based-electroporation where cells are electroporated in the microchannels and under the dynamic flow, and microcapillary-based electroporation where cells are electroporated in controlled reaction chambers and under static flow condition. Focusing on the biological and the challenges of clinical applications, this review article focused on the achievements of microcapillary electroporation earlier than 2009. However, this article did not review the structures and mechanisms of these microfluidics electroporative devices. Most recently, Wang (2010) published a review article focused on the experimental devices of single cell electroporation.

In this article, by going through the current microfluidic devices and their applications, we classify the microfluidic electroporation devices as follows:

- The microfluidic electroporative devices that are used to perform the cell lysis and release the subcellular contents.
- The microfluidic electroporative devices that are utilized for inserting external molecules (transfection) such as DNA and Q-dots (Ho and Kam 2010) into the cells.
- The microfluidic electroporation utilized in other processes such as electrofusion, metabolism monitoring, and localization of Kinases within cells.

In the following sections of this review article, the latest achievements of the microfluidic devices for cell electroporation will be reviewed. Analytical studies are essential to have a better understanding on the functionality of these microfluidic devices, thus the governing equation on the cell membrane permeabilization will be explained first. Focusing on the cell transfection, the currently published analytical and numerical studies on cell electroporation will be reviewed. After that, the recent experimental works on the microfluidic devices of cell electroporation will be evaluated. This review article emphasizes the microfluidic electroporation devices for transfection. Considering cell viability and transfection rate (as the two most important factors of reversible cell electroporation), the effectiveness of the reported microfluidic systems for cell transfection will be compared. At the end, the shortcomings of the current research of microfluidic-based cell electroporation will be summarized and some trends and guidelines will be proposed for future works.

2 Theory of cell permeabilization

The theory of the generation and the development of the pores on the cell membrane due to the applied electric field can be found in a number of articles (Weaver and Chizmadzhev 1996; Krassowska and Filev 2007; Escoffre et al. 2009). This theory is based on the energy minimum principle and valid for the uniformly polarized membrane. Many other studies utilized this approach to investigate the effect of different parameters on cell electroporation such as field strength and rest potential (DeBruin and Krassowska 1999a), ionic concentration (DeBruin and Krassowska 1999b), duration and frequency of electrical shock (Bilska et al. 2000), electroporation of circular cells (Shil 2008; Talele et al. 2010), cellular uptake of macromolecules (Zaharoff et al. 2008), and feedback control of generated pore radii (Cukjati et al. 2007).

According to this theory, there are two kinds of pores in the cell membrane: hydrophobic and hydrophilic (see Fig. 1). The hydrophobic pores are simply gaps in the lipid bi-layer of the membrane that is formed because of the thermal fluctuation. The hydrophilic or inverted pores have their walls lined with the water-attracting heads of lipid molecules. Hydrophilic pores allow the passage of water-soluble substances, such as ions, and thus they conduct electric current while the hydrophobic pores do not.

The pore energy is the required energy to introduce a single pore with radius r to the cell membrane while the other pores are fixed. This energy consists of two parts: $E(r)$ for hydrophilic pores and $U(r)$ for hydrophobic pores.

The hydrophobic pore energy can be calculated as (Neu and Neu 2009):

$$U(r) \approx E_* \left(\frac{r}{r_*}\right)^2 - \frac{1}{2h}(\varepsilon_w - \varepsilon_m) V_m^2 \pi r^2 \quad (2)$$

where radius r_* and energy E_* are the threshold radius between the hydrophobic and hydrophilic pores and the threshold pore energy at r_*, respectively. Pores with $r < r_*$ are hydrophobic, and pores with $r > r_*$ are hydrophilic. h is

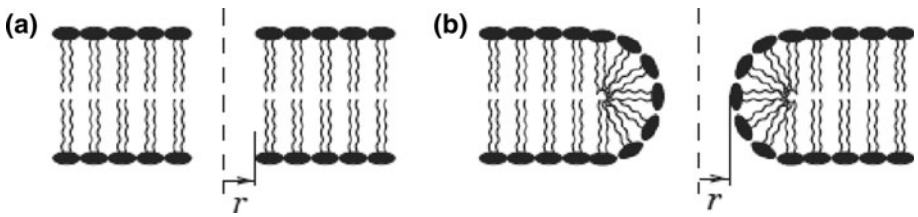

Fig. 1 The structure of **a** hydrophobic and **b** hydrophilic pores created in cell membrane. Pore radius is denoted by r (Neu and Neu 2009)

the membrane thickness, and ε_w and ε_m are permittivity of water and membrane, respectively.

The first term in $U(r)$ represents the energy cost for creating a cylindrical gap of radius r in the membrane and the second term is the effect of the transmembrane potential, V_m, that decreases the energy of membrane by affecting the capacitive energy stored in the membrane.

The hydrophilic energy, $E(r)$ can be calculated by (Neu and Neu 2009):

$$E(r) \approx \beta\left(\frac{r_*}{r}\right)^4 + 2\pi\gamma r - \sigma\pi r^2 - \int_{r_*}^{r} F(r', V_m)\mathrm{d}r' \tag{3}$$

where β and γ are constants, σ is the membrane tension, and F is the electric force. In Eq. 3, the first term represents the electrostatic repulsive force between the lipid heads forming the walls of the pores. Second term is the energy required to bend the bi-layer to form the pore perimeter. The third term represents the decrease in the energy due to the effect of the membrane tension; and the forth term is due to the effect of the transmembrane potential V_m that is derived by evaluating the mechanical work required to deform a dielectric body in an ionic solution with steady state electric current. $F(r, V_m)$ can be calculated by the following equation (Krassowska and Filev 2007). In this equation, F_{max} and r_h are constants.

$$F(r, V_m) = \frac{F_{max}}{1 + r_h/(r + r_h)} V_m^2 \tag{4}$$

The creation of the pores is believed to be two steps. Pores are initially created as hydrophobic pores with radii between r and $(r + \mathrm{d}r)$ at the following rate (per unit area of the membrane) (Neu and Neu 2009):

$$\upsilon_c h \frac{\partial}{\partial r}\left(\frac{U}{kT}\right) e^{-U/kT}\mathrm{d}r \tag{5}$$

where υ_c is the fluctuation rate of the bi-layer per unit volume, k is Boltzmann's constant, and T is absolute temperature.

The pores are initially hydrophobic ($r < r_*$) (r_* is the threshold radius between the hydrophobic and the hydrophilic pores). At $r = r_*$ pores instantaneously changes its configuration (from hydrophilic to hydrophobic) to minimize their energy. The pores with $r > r_*$ are hydrophilic.

As the hydrophobic pores are created, they started to expand or shrink due to two different mechanisms: advection and diffusion. Advection is the definite time rate of change of pore radius, leading to the decreasing of the bi-layer energy; and diffusion refers to the random increases and decreases of the pore radius induced by thermal fluctuation. However, between these two mechanisms, advection is dominant by far. The hydrophilic pore of radius r is assumed to evolve with advection velocity u (Neu and Neu 2009):

$$u = \frac{\mathrm{d}r}{\mathrm{d}t} = -\frac{D}{kT}\frac{\partial E}{\partial r} \tag{6}$$

In the above equation, E is the hydrophilic pore energy, and D is the diffusion coefficient associated with random fluctuation of pore radius.

In order to consider the effect of interfacial energy on pore generation, constant membrane tension in Eq. 3 can be replace by the effective membrane tension (Neu and Neu 2009):

$$\sigma_{eff}(A_p) = 2\sigma' - \frac{2\sigma' - \sigma_0}{\left(1 - A_p/A\right)^2} \tag{7}$$

In this equation, σ' is the interfacial energy per area of the hydrocarbon–water interface, σ_0 is the surface tension of the membrane without pores, A_p is the total area of pores, and A is the area of the lipid bi-layer. Therefore, the advection velocity in Eq. 6 can be approximated as (Neu and Neu 2009):

$$u(r, V_m, A_p) = \frac{D}{kT}\left\{4\beta\left(\frac{r_*}{r}\right)^4\frac{1}{r} - 2\pi\gamma + 2\pi\sigma_{eff}(A_p)r + F(r, V_m)\right\}, \quad \text{in } r \geq r_* \tag{8}$$

As indicated above, the pores are created to minimize the energy. E has two local minima at $r = r_m \approx 1$ nm and at $r = r_s \gg r_m$. It means that pores divided themselves into two different groups, small pores ($r = r_m$) and large pores ($r = r_s$). By removing the external electric field, the transmembrane potential becomes zero; consequently, all the pores shrink to r_m. After that, the pores can reseal by first converting to the hydrophobic configuration and then being destroyed by lipid fluctuations.

Considering the above procedure, the electroporation process can be categorized into five different steps: induction, expansion, stabilization, resealing, and memory. Through the induction step, the transmembrane potential increases until it reaches its critical value. This step is usually takes less than 1 μs. As long as the threshold value of TMP maintains, the number and radius of nanopores increases continuously, this step is usually called expansion. The shape and the duration of electric pulses determine the time span of this step that is usually in the range of microseconds to milliseconds. When decreasing the external electric field to its subcritical value, as long as the nanopores are exit, most cell membranes have a much more normal state that is called stabilization. By removing the external electric field, cell membrane runs into the resealing process that usually spans from second to minutes. After this step, some more resilient changes are

usually remains in cell membrane that takes from minutes to hours. This phase is usually called as memory (Wang 2010).

By considering the physics of pore creation, evolution and resealing, the following advection–diffusion partial differential equation (PDE) can be obtained for the pore density distribution, $n(r, t)$ (Neu and Neu 2009):

$$\frac{\partial n}{\partial t} = D\frac{\partial^2 n}{\partial r^2} - \frac{\partial}{\partial r}(un) + \upsilon_c h \frac{\partial}{\partial r}\left(\frac{U}{kT}\right) e^{-U/kT} - \upsilon_d \eta H(r_* - r) \tag{9}$$

The four terms on the right-hand side in Eq. 8 represent the four mechanisms that causes change in $n(r, t)$:

$D\frac{\partial^2 n}{\partial r^2}$: the diffusion term describes random fluctuation of pore radii caused by thermal energy

$-\frac{\partial}{\partial r}(un)$: the advection term describes the changes in pore radii that are driven by minimization of the energy of the bi-layer; u is the drift velocity. For hydrophilic pores, E is replaced by U in Eq. 6.

$\upsilon_c h \frac{\partial}{\partial r}\left(\frac{U}{kT}\right) e^{-U/kT}$: creation rate of pores (Eq. 5).

$-\upsilon_d \eta H(r_* - r)$: the destruction term describes disappearance of pores; since only hydrophobic pores can be destroyed by lipid fluctuation, this term contains the Heaviside's step function $H(r)$.

Because of the exponential dependence of the creation rate on the pore energy and the existence of disparate spatial and temporal scales, the numerical solution of PDE (9) requires very small discretization steps. To avoid the large computational cost associated with the numerical solution of PDE (9), this equation is asymptotically reduced to a following system of ODE (Neu and Krassowska 1999):

$$\frac{\mathrm{d}N}{\mathrm{d}t} = \alpha e^{(V_\mathrm{m}/V_\mathrm{ep})^2}\left(1 - \frac{N}{N_\mathrm{eq}(V_\mathrm{m})}\right) \tag{10}$$

where $N(t)$ is the density of pores define as:

$$N(t) = \int_{r_*}^{\infty} n(r, t)\mathrm{d}r \tag{11}$$

N_eq is the equilibrium pore density for the given transmembrane voltage, V_m:

$$N_\mathrm{eq}(V_\mathrm{m}) = N_0 e^{q(V_\mathrm{m}/V_\mathrm{ep})^2} \tag{12}$$

For the membrane with k pores, the rate of change of their radii, r_j, can be determined by the following set of equations:

$$\frac{\mathrm{d}r_j}{\mathrm{d}t} = U(r_\mathrm{j}, V_\mathrm{m}, \sigma_\mathrm{eff}), \quad j = 1, 2, \ldots, k \tag{13}$$

In Eqs. 10–12, N_0, q, α, and V_ep are some constants. If the membrane of the cell has k pores, the total current I_p can be computed by adding the currents through all pores:

$$I_\mathrm{p}(t) = \sum_{j=1}^{K} i_\mathrm{p}(r_\mathrm{j}, V_\mathrm{m}) \tag{14}$$

i_p can be computed using the following equation:

$$i_\mathrm{p}(r, V_\mathrm{m}) = \frac{V_\mathrm{m}}{R_\mathrm{p} + R_\mathrm{i}} \tag{15}$$

where R_p is the Ohmic resistance of the cylindrical pores and R_i is the correcting resistance that is used to consider the effect of changing in transmembrane potential in vicinity of the pores.

$$R_\mathrm{p} = \frac{h}{s\pi r^2} \tag{16}$$

$$R_\mathrm{i} = \frac{1}{2sr} \tag{17}$$

The above-reviewed theory is the most widespread analytical approach to study the effect of electric field on the pore creation in the cell membrane. Many studies utilized this theory to investigate different aspects of cell electroporation. Although the above theoretical model can address many aspects of cell electroporation, there are some shortcomings associated with it:

- First, this model can not explain the mechanism of resealing the pores with radius $r \geq r_\mathrm{m}$.
- The effect of changing volume of the cell is not considered in the above analysis. Many studies show that in the presence of external electric field, the cells started to deform from circular to elliptical shape (Teissie et al. 2002), and to expand (Wang et al. 2006b) or rotate (Gimsa 2001). For example, previous experimental studies show that in the presence of external electric field, the cell can expand up to 300% of its original volume (Wang et al. 2006b).

3 Early studies on reversible cell electroporation

One of the most interesting applications of microfluidic electroporation are cell transfection. Reversible cell electroporation and DNA electrotransfer trace its roots to 1982 (Neumann et al. 1982). At the beginning of the millennium, the idea of using microfluidic devices for electroporation initiated. In a series of publications, Huang and Rubinsky (2000, 2001, 2003) presented their microfluidic electroporation device. In fact, this is the first practical attempt to use microfluidic devices for cell electroporation purpose. Figure 2 shows the schematic diagram and optical image of this work. The electroporation system contains one microchannel with a approximate width equal to 1.5 times of the cell diameter. In this way, the cells are forced to pass

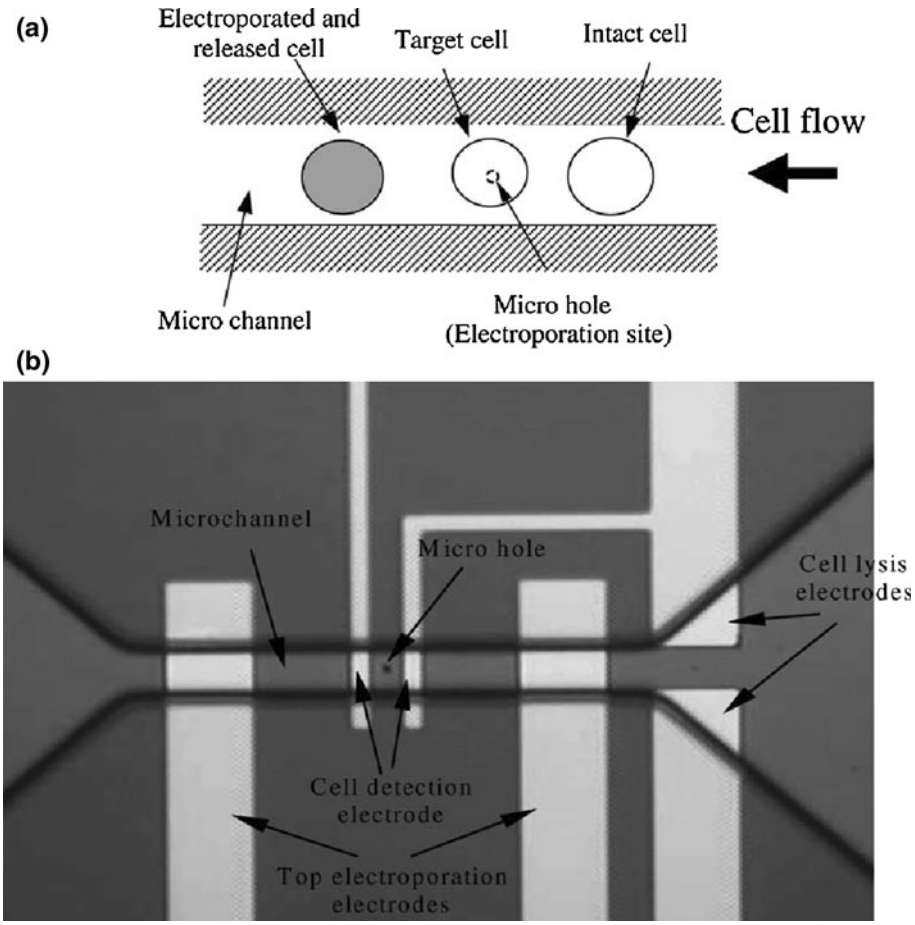

Fig. 2 **a** Scheme of the first proposed flow-through micro-electroporation chip. **b** Optical image of the layout the first microfluidic electroporation device. Micro-hole, micro-channel, and integrated electrodes are tagged in this picture (Huang and Rubinsky (2003)

through the channels one by one and electroporated individually (single cell electroporation). There is a hole at the center of this channel. The purpose of the hole is to trap the cells and fixes them during the electroporation process. Three pairs of electrodes are used in this system. The function of one set of electrodes at the entrance of channel is to prevent the large cells from entering the channel. This was achieved by producing electrical repelling force against the large cells. Two 10-μm wide auxiliary micro-electrodes were placed 10-μm away on both sides of the microhole for cell detection by impedance measurement. Two other electrodes were placed 100-μm apart on two sides of the micro-hole to generate the required electric field for performing electroporation. The cells flew through the channels one by one were trapped by the micro-hole and electroporated. By applying 10-V electric potential with 10-ms duration, this system is used to reversibly electroporate the Human prostate adenocarcinoma cells (ND-1 cell line). It was reported that the cell transfection efficiency of this system is 100%.

The other leading works in the field of microfluidic electroporation was conducted by Shin et al. (2004). The electroporative device is simple and consists of one microchannel connecting two reservoirs for the inlet and the outlet on a PDMS chip. The electrodes were inserted at the two reservoirs. The flowing cells through the channel were electroporated by the applied voltages between the two electrodes. Using this system, the EGFP could be transfected into the SK-OV-3 cells in a 0.4-kV/cm electric field; while the same transfection process was performed in the conventional electroporator at the 1-kV/cm electric field.

4 Analytical studies on cell electroporation

Before reviewing the experimental set-ups for microfluidic cell electroporation, it is worthy to have a look at some important analytical studies on microfluidic cell electroporation. Although the current analytical studies are unclear regarding the exact mechanisms of ions and macromolecule exchange across the cell membrane, they present some interesting clues for future works. The underlying concept in many of these analytical studies is the "theory of cell permeabilization" that was explained in Sect. 2. These studies can be categorized in three different groups:

1. The studies investigated the effects of different parameters such as field strength, ionic concentration,

pulse strength and duration on the cell permeabilization.
2. The studies conducted to evaluate the uptakes of fluid, ions and macromolecules by the cell during the electroporation.
3. Studies focused on optimizing and controlling of electric pulse during the cell electroporation.

4.1 The studies investigated the effects of different parameters such as field strength, ionic concentration, pulse strength, and duration on the cell permeabilization

Many studies employed the above-mentioned analytical approach to study the cell electroporation. In these studies, Laplace equation was solved in order to find the electric potential inside (Φ_i) and outside (Φ_e) the cell. Equation 18 was suggested to find the current density across the cell membrane (DeBruin and Krassowska 1999b). In this equation, cell membrane is modeled as a parallel capacitor and resistance system. Transmembrane potential (V_m or *TMP*) is defined as: $V_m = \Phi_i - \Phi_e$. In the equation below, I_{ion} is the ionic current, and I_{ep} is the current due to electroporation.

$$-\hat{n}\cdot(\sigma_i\nabla\Phi_i) = -\hat{n}\cdot(\sigma_e\nabla\Phi_e) = C_m\frac{\partial V_m}{\partial t} + I_{ion} + I_{ep} \quad (18)$$

Using this approach, in a series of articles DeBruin and Krassowska (1999a, b) studied the effect of field strength, rest potential and ionic concentration on the cell permeabilization. According to their results, V_m (transmembrane potential) is symmetric about the equator with the same value at both poles of the cell. Larger shocks do not increase the maximum magnitude of V_m because more pores form to shunt the excess stimulus current across the membrane. In addition, the value of the rest potential does not affect V_m around the cell because the electroporation current is several orders of magnitude larger than the ionic current that supports the rest potential. Once the field is removed, the shock-induced V_m discharges within 2 s, but the pores persist in the membrane for several seconds. Complete resealing to pre-shock conditions requires approximately 20 s.

Bilska et al. modeled electroporation in two geometries, a space-clamped membrane and a single cell, and investigated the effects of pulse duration, frequency, shape, and strength. The effectiveness of each shock is measured by the fractional pore area (FPA). The results indicate that FPA is sensitive to shock duration only in a very narrow range. In contrast, FPA is sensitive to shock strength and frequency of the pulse train, increasing linearly with shock strength and decreasing slowly with frequency. Their results indicate that varying the strength and frequency of a monophasic pulse train is the most effective way to control the creation of pores (Anna O. Bilska et al. 2000).

Mossop et al. (2007) investigated that how the intracellular field is altered by electroporation. In their study, they showed that the intracellular current could vary several orders of magnitude, whereas the maximum variations in the extracellular and total currents were less than 8 and 4%, respectively. A similar difference in the variations was also reported when comparing the electric fields near the center of the cell and across the permeabilized membrane, respectively. According to their results, electroporation also caused redirection of the extracellular electric field that was significant only within a small volume near the permeabilized regions, suggesting that the electric field can only facilitate passive cellular uptake of charged molecules near the pores. Within the cell, the field was directed radially from the permeabilized regions, which may be important for improving intracellular distribution of charged molecules.

Neu and Neu (2009) presented a model of electroporation in a spherical cell exposed to an electric field. Using the mentioned analytical study in Sect. 2, they investigated the pore density around the cell for one case of study. According to their results, the highest pore density occurs on the depolarized (the nearest point on cell membrane near negative electrode) and the hyperpolarized (the nearest point on cell membrane near positive electrode) poles but the largest pores are on the border of the electroporated regions of the cell. Despite their much smaller number, large pores comprise 95.3% of the total pore area and contribute 66% to the increased cell conductance. For stronger pulses, pore area and cell conductance increase, but these increases are due to the creation of small pores; the number and size of large pores do not increase (Krassowska and Filev 2007).

Talele et al. (2010) developed a numerical model for single and spherical cell electroporation. They simulated spatial and temporal aspects of the transmembrane potential and pore radii as an effect of applied electric field. Based on their results, that pore radii tend to be more normalized for AC fields. The relative difference in FPA is reduced by the use of a 1-MHz sinusoidal applied electric field over a 100-kHz field.

These numerical and analytical studies on cell electroporation have some underlying assumptions. First, they assumed the spherical cells. However, some studies indicated that in the presence of applied electric field, cells deform from spherical to elliptical shape (Teissie et al. 2002). Second, they considered the cells in an infinite space. However, in microfluidic electroporation, cells are usually located in the microchannels or micro-chambers.

The results of these studies may not reflect the boundary effects of microfluidic based electroporative devices. Furthermore, the effects of cell expansion and rotation during the electroporation are not considered. More sophisticated analytical models are needed to investigate the effects of electro-deformation including swelling and rotation.

4.2 The studies conducted to evaluate the uptakes of fluid, ions, and macromolecules by the cell during the electroporation

A few studies were conducted on the mass transfer and uptake rate into the cells during the electroporation. There are not any accurate models that consider electrokinetic effects on the mass transfer through the nanopores in cell membrane. Furthermore, most of the current studies are based on continuum hypothesis that may become invalid in the small dimensions of nanopores.

Zaharoff et al. (2008) used one-dimensional mass transfer equation to compute the cellular uptake of macromolecules. This study utilized the analytical approach as explained in Sect. 2 to estimate the dimension of the generated pores due to the applied electric field in the cell membrane. They treated these pores as a channel to uptake the macromolecules to the cell. They considered only the effect of diffusion in this process and their analysis was based on continuum hypothesis. However, they concluded that continuum assumption used in their mathematical modeling is improper for simulating diffusion within the cell; convection is probably the dominant mechanism of transport for cellular uptake of uncharged macromolecules; in addition, the effect of electrophoresis must be considered in the cellular uptake of highly charged molecules. Another important effect on cellular uptake is cell deformation that was ignored in this study.

Another study conducted by Granot and Rubinsky (2008) numerically investigated the delivery of drugs into the tissue cells by electroporation. This study was based on the following assumptions: the process of mass transfer happens in every cell in the tissue; the cells are infinitesimally small; and that the drug entering the cell can be modeled as a uniformly distributed reaction rate. They further assumed that the cells are uniformly packed in the tissue so that each spherical cell is contained in a cube whose edge is equal to $2r$. They also considered only the effect of diffusion. In this study, first by employing the analytical approach explain before (Neu and Neu 2009), they attributed to each cell at any location in the tissue a lumped value of permeability to drug which is proportional to the local value of the electrical field. After that, by only considering diffusion as an uptake mechanism, the mass-transfer equation, Eq. 19, was solved to find the concentration distribution of drug in the tissue in the reversible electroporation. The reaction rate (R) can be computed as $R = J(A_p/V_0)$ where A_p is the pore cross-sectional area of the permeable cells in each point of the tissue, $V_0 = (2r)^3$ is the volume of cube surrounded the cell, J is flux per area that can be estimated by using Fick's law: $J = -P\ (c_{ex} - c_{in})$, where P is the permeability of the drug molecules through the membrane pores.

$$\frac{\partial c}{\partial t} - \nabla(D\nabla(c)) = R \tag{19}$$

Because of transmembrane potential, electrokinetic effects most probably play a role in the cell uptake during electroporation. So far the electrokinetic effects on transport processes in nanochannels have not been investigated adequately yet. The created nanopores in cell membrane during the electroporation can be viewed as nanochannels. Extensive researches are required to understand the electrokinetic transport of fluid, ions, and macromolecules through nanochannels.

4.3 Studies focused on optimizing and controlling of electric pulse during the cell electroporation

Effect of electric pulse shape on the electroporation efficiency is important. Different pulse shapes can generate various effects on the cell (Fox et al. 2006). Some studies investigated the effect of different pulse shapes (Sinusoidal, step, and triangular) on the transmembrane potential and the number of the pores. For example, Talele et al. (2010) showed that as long as a threshold of transmembrane potential is maintained by the electric field, pore density is increases. They also showed that the bipolar pulses leads to the asymmetrical pore density between the two cell polar regions. In 2010, Miklavcic and Towhidi proposed an analytical model to predict the effects of arbitrarily shaped electroporation pulses on cell membrane conductivity and on molecular transport across the cell membrane. Knowing electrical and diffusion properties of the cells and the specific dye, their proposed model can be used to optimize of the electroporation protocol.

Other studies in this category used feedback control techniques to reduce the side effects of electric pulse on cell structure. Experimental studies showed that feedback control improves the electroporation efficiency of single cells (Cukjati et al. 2007; Khine et al. 2007). Feedback control can ensure the safe and accurate transfection during the reversible electroporation by monitoring the radii of the pores and the time duration for which the pores remain open. So far some experimental studies have been reported on the feedback control of the single cell electroporation cells (Cukjati et al. 2007; Khine et al. 2007). The interest of performing analytical studies on feedback control of cell electroporation increases recently. Because of nonlinear

behavior of the cell electroporation, many conventional controllers cannot be exploited. One of the first analytical studies on the closed loop control of the cell electroporation was conducted by Zhao et al. (2010). Using a nonlinear control technique, they regulate the input voltage to stabilize the generated pore radii around the desired value. However, their design control theory is based on some nonlinear mathematical analysis that may be hard to implement. Other user-friendly control techniques (for example fuzzy logic) can be utilized to control the electroporation process.

5 Experimental studies on cell electroporation

As it is mentioned in Sect. 1, the experimental studies of microfluidic cell electroporation have three main applications: cell lysis and releasing the subcellular contents of the cells, cell transfection, and other applications that utilize cell electroporation as a part of the process such as electrofusion and metabolism monitoring. In this section, we focus on the mechanical structure, mechanism and performance of the microfluidic electroporation devices proposed after 2005. For the microfluidic electroporation devices prior to 2005, readers may refer to the review article on microfluidic cell electroporation by Fox et al. (2006). The technical, biological, and electrical properties of these microfluidic devices are summarized in Tables 1, 2, and 3.

5.1 Microfluidic electroporation devices for cell lysis (irreversible electroporation)

Analysis of the intercellular contents is essential for many biological cell studies. In the microfluidic electroporation devices, cell lysis usually accomplish in microchannels and under a dynamic flow field. This may facilitate the removal of subcellular contents and cell debris. One of the leading studies that suggested using continuous flow in microchannels with varying geometry for electroporation carried out by Lu et al. (2005). Figure 3 shows the schematic diagram of this microfluidic electroporation system. This system contains vertical saw-tooth electrode on the two opposite sides of the channel wall. Using the saw-tooth shape electrode, the induced electric field could be intensified periodically along the channel. The duration of these electric pulses is tuned by the flow field velocity and geometry of the electrode-channel system. This system utilize thick electrode that last longer in the corroding environment. In spite of planar electrodes, vertical electrodes can generate a uniform electric field in the system. This study also suggested using AC electric field instead of DC to reduce bubble creation and pH changes in vicinity of electrodes. The more specific characteristics of the designed system and electroporation mechanism have specified in Tables 1, 2, and 3. Their results show that by applying a 6 V–AC electric field with 5-kHz frequency, 28% of cells are lysed completely while 81% of cells are partially lysed; their membrane did not disrupted completely and they just loss some parts of their organelles and cytosolic material during electroporation. In this system, the percentages of complete and partial cell lysis become 74 and 71 for a 8.5 V–AC electric field with 10-kHz frequency, respectively.

In 2006a, b, c, Wang et al. proposed applying continuous DC voltage along the microchannel with variable cross-section for electric pulse generation. Schematic diagram of this system has been show in Fig. 4. The continuity of the electric current density leads to a stronger electric field in the narrower cross-sections of the channel. In this mechanism, the cell velocity and dimensions of the system can adjust the duration of the generated electric pulses. The distinguished characteristic of this study is the direction of applied electric field. This is the first work that applies electric field along the channel. This mechanism has many advantages. Its auxiliary instruments are very simple. There is no need for pulse generator. It needs only a simple DC power supply and the pulse is generated by the geometric alteration. No microscale electrodes or subcellular structures needed. The low-cost and simple microfabrication procedure (such as soft-lithography) can be utilized to fabricate the chip. In addition, the narrow electroporative part of the channels allows having a single-cell electroporation. This also presents the ability of on-line monitoring during the electroporation process. Above all, the presence of external electric field along the channel causes electrokinetic effects that can facilitate many pre- and post-processing requirements. For example, electroosmosis effect can generate the flow in the channels of the system, or electrophoresis force can be utilized to manipulate the cells in the system.

Using this system, the electroporation carried out on Chinese hamster ovary (CHO) cells with diameters ranging from 10 to 16 μm. The results of this study include several parts. First, they showed that the cells start expanding in the continuous electric field. In order to study the effect of electric field on the cell, they increased the electric field from 0 to 1200 V/cm. To study the internalization of dye SYTOX, they increased E (external electric field) keeping the pulse duration equal to 40 ms. Their results showed that when E is below 400 V/cm, there is not any significant dye internalization or cell death. When E is higher than 400 V/cm, cell electroporation is initiated. According to their findings, at $E = 500$ V/cm, about 56% of cells are reversibly electroporated. In fact, the best efficiency of dye internalization takes place at $E = 500$ V/cm. Above this value, the rate of

Table 1 Technical property of electroporative devices

References	Materials	Focusing type	Typical size	Electrode material	Electrode distance	Flow type
Lu et al. (2005)	Pyrex 7740	Geometry variation	30–130 μm	Gold	30–130 μm	PDF
Wang et al. (2006a)	PDMS	Geometry Variation	33–213 μm	Pt Wire	Far (~7 mm)	PDF
Wang et al. (2006a, b, c)	PDMS	Geometry variation	25–219 μm	Pt Wire	Far (~10 mm)	EKF
Wang et al. (2006b)	PDMC	Geometry variation	33–213 μm		Far (7 mm)	PDF
Wang and Lu (2008)	PDMS	Geometry variation	62.5–500 μm	Pt Wire	Far (4–5 mm)	PDF
Bao et al. (2010)	PDMS	Geometry variation	58 μm–5 mm	Pt Wire	Far (12–25 mm)	PDF
Kim et al. (2007)	PDMS	Salt bridge	40–500 μm	Ag/AgCl	Far	PDF
Ikeda et al. (2007)	Pyrex 7740	Geometry variation	50 μm–100 μm	Pt/Ti	50 μm	EKF
Khine (2005a, b)	PDMS	Cell trapping Negative pressure	3.1 μm	Ag/AgCl	Far	PDF
Valero et al. (2008)	Silicon-glass	Cell trapping Negative pressure	4, 20, 50 μm	Pt Wire	~17 μm	PDF
Wang et al. (2007)	PDMS/glass	Elastomeric valve	200 μm	N/S	Far	N/S
Fei et al. (2007)	PMMA	Cell trapping Negative pressure	500 μm	Silver	Far	EKF
Suzuki et al. (2007)	Glass	Cell trapping Negative pressure	2 μm	N/S	Far	PDF
Cao et al. (2008)	Silicon	–	80 μm	Ti/Gold	50–100 μm	PDF
Sedgwick et al. (2008)	PDMS	Cell trapping Dielectrophoresis	100 μm	Ti/Gold	10 μm	PDF
Khine et al. (2007)	PDMS	Cell trapping Negative pressure	N/S	Ag/AgCl	Far	PDF
Luo et al. (2006)	PDMS	Microfluidic droplet	30–300 μm	Au	20 μm	PDF
Zhan et al. (2009)	PDMS	Microfluidic droplet	60–386 μm	Gold	20 μm	PDF
Huang and Rubinsky (2003)	Silicon/glass	Cell Trapping Negative pressure	30–500 μm	Pt/Cr	10–100 μm	PDF
Shin et al. (2004)	PDMS	No focusing	100–500 μm	Pt	Far (2 cm)	PDF
Vassanelli et al. (2008)	Silicon	No focusing	–	Gold	150–300 μm	No flow
Lim et al. (2009)	Glass	No focusing	10 mm	ITO	10 mm	N/S
Lee et al. (2006)	Silicon	No focusing	–	Pt, Ag/AgCl	Near	No flow
Valley et al. (2009a)	Glass	By light	255 μm	Virtual	Near	PDF
Zhu et al. (2010)	PDMS	Hydrodynamics	50–150 μm	Ag	Far	PDF

PDF pressure-driven flow, *EKF* electrokinetic flow, *PMMA* polymethylmethacrylate, *ITO* indium tin oxide electrode

cell death is increased. At $E = 800$ V/cm almost all cells are dead. This article also includes studies on the effect of two main parameters affecting the cell viability in electroporation: the duration and the intensity of electric pulse. Based on their results, if E is less than 400 V/cm (the threshold of electroporation), the cell will be viable even for long duration pulses. For higher values of electric field, the cell viability is much more sensible to pulse duration. Their experimental results show that for $E = 600$ V/cm, almost all the intercellular contents will be depleted after 150 ms. The required time for complete cell lysis reduces to 60 ms for $E = 1000$ V/cm and 30 ms for $E = 1200$ V/cm. From the findings of this article, one can concluded that for cells with diameter ranging from 10 to 16 μm, if the applied electric field is between 0 and 400 V/cm, no electroporation will occur and almost all the cells will remain viable. Cell lysis starts at 600 V/cm. Cell internalization accomplishes at the applied electric fields between 400 and 600 V/cm. The best efficiency of cell internalization will be happened at 500 V/cm and almost 56% of the cells remain viable after electroporation.

Using the mechanism proposed by Wang et al. (2006a), Bao et al. (2008) suggested conducting the selective intercellular release. They showed that in general calcein was released at lower field intensities and shorter durations than did SykEGFP (72-kDa protein kinase, Syk, tagged by enhanced green fluorescent protein (EGFP) from chicken B cells). By tuning the electric pulse intensity and duration

Table 2 Electroporated cell properties

References	Purpose	Species	Cell type	Cell size	Moving or stationary cells	Single or multi cells
Lu et al. (2005)	Cell lysis	Human	HT-29	10 μm	Moving	Single
Wang (2006a)	Cell lysis and transfection	Hamster	CHO	10–16 μm	Moving	Single
Wang et al. (2006a, b, c)	Lysis	Bacterial	*E. coli*	N/S	Moving	Multi
Wang et al. (2006b)	Swelling/lysis	Hamster	CHO	10–16 μm	Moving	Single
Wang et al. (2008)	Transfection	Hamster	CHO	10-16 μm	Moving	Multi
Bao et al. (2010)	Swelling/Lysis	Mouse	RBC	–	Moving	Multi
		Mouse	WBC	–		
		Mouse	M109, CTC	–		
Kim et al. (2007)	Transfection	Human	K569	–	Moving	Single
Ikeda et al. (2007)	Cell lysis	Plant	Zucchini protoplast cells	40–85 μm	Moving	Single
Khine (2005a, b)	Transfection	Human	HeLa Cell	10 μm	Stationary	Single
Valero et al. (2008)	Transfection	Mouse	C2C12[a]	–	Stationary	Single
		Human	MSCs	–		
Wang et al. (2007)	Transfection	Hamster	CHO	10–16 μm	Stationary	Multi
Fei et al. (2007)	Transfection	Mouse	NIH 3T3[b]	–	Stationary	Multi
Suzuki et al. (2007)	Transfection	Human	HeLa Cell	–	Stationary	Multi
Cao et al. (2008)	Electrofusion	Human	HEK-293	–	Moving	Multi
		Plant	CMP	–		
Sedgwick et al. (2008)	Cell lysis	Human	A431 squamous cell	–	Stationary	Single
Khine et al. (2007)	Transfection	Human	HeLa Cell	–	Stationary	Single
Luo et al. (2006)	Transfection	Plant	Yeast cells	–	Moving	Single
Zhan et al. (2009)	Transfection	Hamster	CHO	–	Moving	Single
Huang and Rubinsky (2003)	Transfection	Human	ND-1 cell line[c]	–	Stationary	Single
Shin et al. (2004)	Transfection	Human	SK-OV-3	10 μm	Moving	Multi
Vassanelli et al. (2008)	Transfection	Hamster	CHO	–	Stationary	Single
Lim et al. (2009)	Lysis	–	FITC-BSA-laden vesicle	1–50 μm	Stationary	Single
Lee et al. (2006)	Transfection	–	Vesicle	10 μm	Stationary	Single
Valley et al. (2009a)	Transfection	Human	HeLa cells	10 μm	Stationary	Single
Zhu et al. (2010)	Transfection	Yeast	–	–	Moving	Single

CHO Chinese Hamster ovary cell, *RBC* read blood cells, *WBC* white blood cells, *CTC* circulating tumor cells, *K569* human chronic leukemia cell, *HEK-293* human embryonic kidney cells, *CMP* plant cucumber mesophyll protoplasts, *MSC* mesenchymal stem cell

[a] Mouse myoblastic cells

[b] Mouse embryonic fibroblast cell line

[c] Human prostate adenocarcinoma cells

(which can be done easily by modifying the geometry and cell velocity in the proposed system; Wang et al. 2006a), one specific intercellular content can be released while the others remain in the cell. Using their suggested electroporation microfluidic device (Wang et al. 2006a), Wang et al. (2006c) could lysis one kind of bacterial cell, *E. coli*. *E. coli* cell is much smaller than mammalian cells. Because the transmembrane potential linearly depends on the cell diameter, the *E. coli* cells required higher values of applied electric field for electroporation rather than mammalian cells. The results of this study show that the local electric field of 1000–1500 V/cm is required for nearly 100% cell death. In this range, the irreversible pores appear in the membrane of the cells that are sufficient for cell lysis. They also showed that for the field strength higher than 2000 V/cm, the cell membrane completely disintegrated.

The main difference between the mechanisms of this study and their previous study is the type of flow field. In this study, they suggested using electrokinetic effects to move the cells and generate flow field. By increasing the applied voltage to the system, on one hand the electric pulse is intensified, on the other hand the cell velocity increases and consequently the pulse durations is decreased (the pulse duration is calculated by the length of electroporative section and cell velocity). Therefore, there is only one degree of freedom in the system, which means

Table 3 Electrical properties of the different electroporation microdevices

References	Purpose	Pulse type	Electric potential range	Pulse duration	Frequency	Generated electric field (kV cm^{-1})
Lu et al. (2005)	Cell lysis	AC	6, 8.5 V	–	5, 10 kHz	0.204–4.65
Wang et al. (2006a)	Cell lysis and transfection	DC	0–200 V	10–100 ms	-	Up to 1.2
Wang et al. (2006a, b, c)	Lysis	DC	0–930 V	Up to 45 s	–	Up to 2
Wang et al. (2006b)	Swelling/lysis	DC	–	Up to 150 ms	–	Up to 1.2
Wang et al. (2008)	Transfection	DC	41–110 V	0.2–20 ms	–	0.3–0.8
Bao et al. (2010)	Swelling/lysis	DC	–	100–300 ms	–	Up to 1.6
Kim et al. (2007)	Transfection	DC	7–20 V	0.8–8 ms	–	0.6–1.8
Ikeda et al. (2007)	Cell lysis	DC[a]	Up to 30 V	–	–	–
		AC[a]	Up to 70 V	–	Up to 1 MHz	–
Khine (2005a, b)	Transfection	DC	0.51 ± 0.13 V	6.5 ms	–	–
Valero et al. (2008)	Transfection	DC	2 V	6 ms	–	0.67
Wang et al. (2007)	Transfection	DC	200–1000 V	20–30 ms	–	
Fei et al. (2007)	Transfection	N/S	N/S	500 ms	1 Hz	0.035
Suzuki et al. (2007)	Transfection					
Cao et al. (2008)	Electrofusion	DC		20–50 μs	–	3.7
Sedgwick et al. 2008)	Cell lysis	AC	Up to 20 V	N/S	100 kHz–1 MHz	1
Khine et al. (2007)	Transfection	DC	0–1 V	5–60 ms	–	N/S
Luo et al. (2006)	Transfection	AC	18 V		1 kHz	–
Zhan et al. (2009)	Transfection	DC	5–9 V	0.37–21.6 ms	–	–
Huang and Rubinsky (2003)	Transfection	DC	10 V	100 ms	–	–
Shin et al. (2004)	Transfection	–	–	10 ms		0.25–0.75
Vassanelli et al. (2008)	Transfection	DC	0.9, 1.3, and 1.7 V	5 ms, 10 ms	–	–
Lim et al. (2009)	Cell lysis	AC	2–5 V	N/S	20 Hz–1 kHz	N/S
Lee et al. (2006)	Transfection	DC	Up to 2 V	Up to 1.5 S	–	–
Zhu et al. (2010)	Transfection	DC	0.5–2.5 V	2.2–11.7 ms	–	0.65–1.87 $kVcm^{-1}$

[a] There are two sets of electrodes in the system. The DC voltage is applied at the outer electrodes to generate the electroosmotic flow while the AC voltage is applied at the inner electrodes for cell lysis

that pulse magnitude and duration could not modify independently.

Figure 5 shows the schematic diagram of the electroporation device proposed by Ikeda et al. (2007). This system consists of two reservoirs that are connected by one flow channel. There is a pinched structure at the center of the channel. Two pairs of electrodes are used in this study. The outer electrodes locate at the end of channels (at reservoirs) and the inner electrodes situate at the center of channels. The outerelectrodes are used to generate the EOF in the system, while the function of the inner electrodes is to generate the required electric field for electroporation. The pinched structure is used to capture the cells between two inner electrodes. Two different pinched structures were used in the system: triangular and trapezoidal. Because of point tips, the cells experiences much more electrical damage in the triangular structure than in the trapezoidal pinched structure.

In this study, cell lysis was performed by both mechanical force (shear force) and electrical means. In their first step of the experiments, the triangular pinched structure was used. The voltage was only applied at the outer electrodes to generate the electroosmotic flow and drive the cells into the pinched structure. In this step, the cells were lysed by the shear force at the triangular pinched structure. Although their results show the effectiveness of this method, there are some limitations with this mechanism. Because cell lysis is carried out by physical contact between the cells and the point tips of the pinched structure, the minimum cell diameter is restricted by the width of the triangular pinched structure. In this method, the flow field and cell movement are caused by the applied electric field. However, the applied potentials at the outer electrodes are restricted by the bubble generation and Joule heating. Because the outer electrodes are only used for flow generation and does not have any contribution in the cell lysis, using other types of micropumps may be much more advantageous. In the second step, the voltage was applied at both inner and outer electrodes. The DC voltage at outer electrodes causes the flow movement while the AC voltage

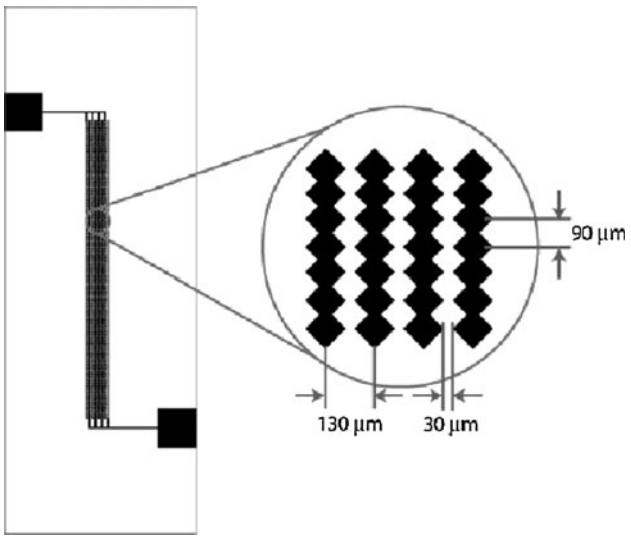

Fig. 3 Schematic diagram and dimensions of the electroporative device suggested by Lu et al. (2005)

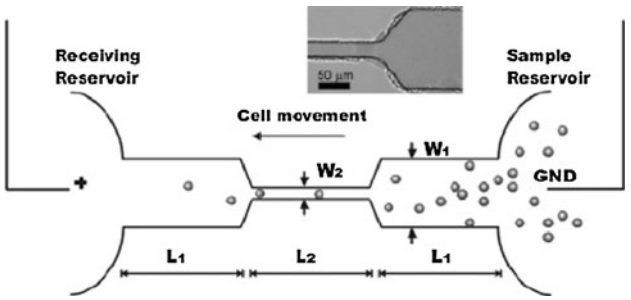

Fig. 4 Schematic diagram of the electroporative device proposed by Wang et al. (2006a). In the electroporative section, the cross-section area of the channels reduces in order to intensify the external electric field

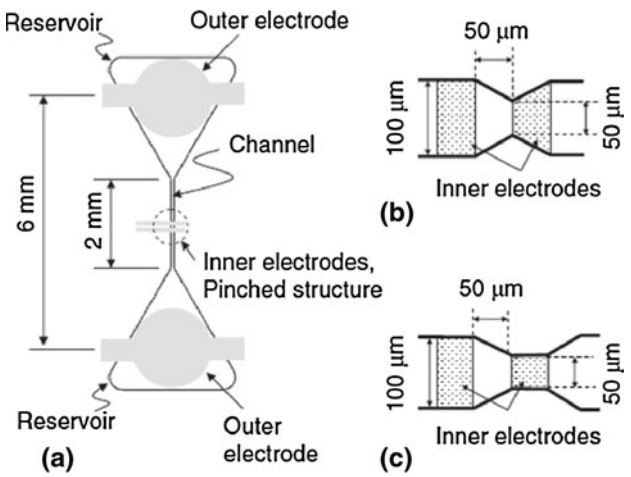

Fig. 5 The channel structures of the microfluidic electroporation device proposed by Ikeda et al. (2007) for cell lysis **a** overview, **b** triangular pinched structure, **c** trapezoidal pinched structure

applied at the inner electrodes resulted in the electrical cell lysis. In this step, both types of the pinched structure were utilized. The electrical parameters at the inner electrodes (applied voltage and frequency) were tuned to lysis the cells. Cell lysis was recorded at the frequencies of 5 kHz to 1 MHz. For one specific applied voltage, lower range of frequencies will result in the bubble generation while the cell can be lysed at the higher range of frequencies. They also experimentally showed that larger cells will electroporate at the lower ranges of applied voltages. This is because the transmembrane potential linearly depends on the cell diameter. It must consider that if the cell diameter is larger than the width of the pinched structure, the pinched type becomes important. Because in these cases the physical contact can also play a role in the cell lysis. In the second method (when the voltage is applied at the inner electrodes), there is no restriction on the minimum cell diameter. However, outer electrodes also does not have any influence on the cell lysis and should be replace by other types of micropumps to reduce the joule heating and bubble generation.

One of the first studies to use dielectrophoretic force for cell trapping in electroporation process was performed by Sedgwick et al. (2008). Other studies have suggested trapping the cells in the fixed position during the cell transfection application using negative pressure. The scheme of the system proposed by Sedgwick et al. is shown in Fig. 6. The system consists of two inlets and one outlet. One inlet is used for cell suspension and the other is used for buffer solution or microsphere injection. The microspheres are used for separation of subcellular contents. One saw-tooth gold microelectrode was positioned perpendicularly to the channel. The electrode exerts AC-voltage to generate dielectrophoretic force (for cell trapping) and to perform cell lysis.

The results show that 20 V AC voltage with 1-MHz frequency can generate the required electrophoretic force to hold the cells against the flow field up to 30 ml/min and without performing cell lysis. Following the trapping step, the frequency was reduced to 100 kHz to perform the cell lysis. For one specific applied voltage, the cell will be trapped at a high frequency (e.g., 800–1000 kHz for 20 V). By decreasing the frequency, the dielectrophoretic force decreases while the cell lysis initiates (for example, at the applied voltage of 20 V and for the frequency range between 200 and 80 kHz, both trapping and cell lysis take place simultaneously). By lowering the frequency, the dielectrophoretic force becomes weaker and can be neglected (for example at the applied voltage of 20 V and with 200-kHz frequency, cells starts to lysis without trapping). At the very low range of frequencies and applied voltage, none of these effects will happen (for example, for the applied voltage below 13 V and for all ranges of

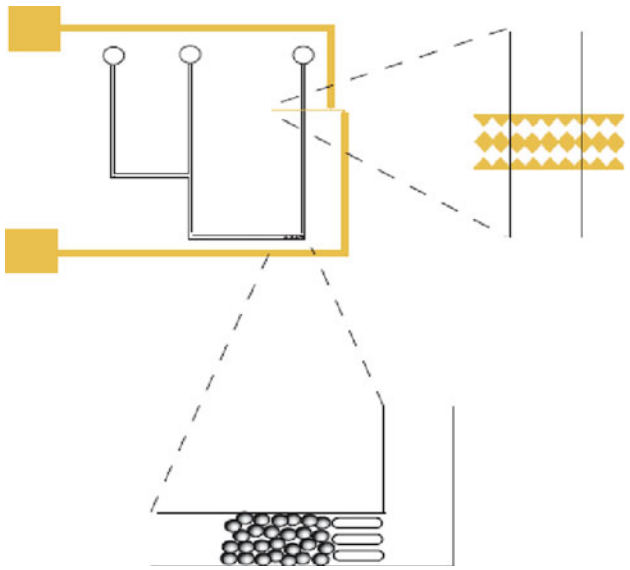

Fig. 6 Schematic diagram of the electroporation microfluidic system proposed by Sedgwick et al. (2008) for cell lysis

frequencies). Their study recorded the cell expansion after trapping and before cell lysis. It was believed that this expansion is due to the osmotic pressure. In the post-processing step, the cell debris and subcellular contents are separated using microspheres. Three obstacles were used in the channels to trap the microspheres. This section is used to separate the cell debris and its intercellular contents.

Another study that used dielectrophoretic force to trap and fix the cells at the predefined positions was conducted by Lim et al. (2009). Figure 7 shows the schematic diagram of this system. There is an electrode at the lower wall of the channel that consists of 16 30-μm wide indium tin oxide (ITO) strips each having a thickness of 0.11 μm and separated by 120-μm bare glass. The upper wall is the uniform ITO-coated glass plate. Two types of electric field arrangement were applied to the system: normal (Fig. 8) and co-planar (Fig. 9). The distance between the upper and

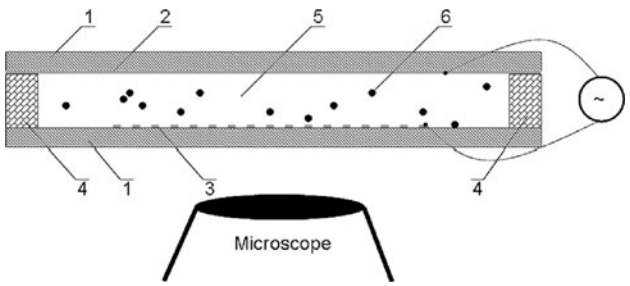

Fig. 7 Schematic illustration of the microfluidic devices proposed by Lim et al. (2009) for cell manipulation and electroporation The tagged sections are: (*1*) glass slide, (*2*) uniform ITO electrode coating, (*3*) 16 ITO microelectrode strips with 30-μm width and 120-μm inter-strip spacing, (*4*) one-millimeter thick polytetrafluoroethylene spacer, (*5*) electrolyte solution, (*6*) colloidal suspension

the lower walls are 10 mm. The FITC-BSA-laden vesicles are used to study the effectiveness of the proposed system for cell lysis. The first step was to position the vesicles near the lower micropattern electrodes. To do this, the normal electric field arrangement (Fig. 8) was utilized. The 2.0 V_{rms} AC voltage with the frequency range of 10–20 kHz was applied to dielectrophoretically manipulate the vesicles and align them along the ITO electrode strips. For one specific applied voltage, the elevation of the trapped vesicles from the bottom surface was determined by the volume of the vesicle. After trapping the vesicles, the normal electric field (Fig. 8) was switched to the co-planar arrangement (Fig. 9) at 5 V_{rms} and 40 Hz to rupture the trapped versicles.

The idea of using dielectrophoresis force to trap the cells during the cell lysis is beneficial. In this way, cells can be suspended and fixed in the flow field. During the cell lysis process, release of the intercellular contents is carried out with the flow to the desired position, while the cell debris

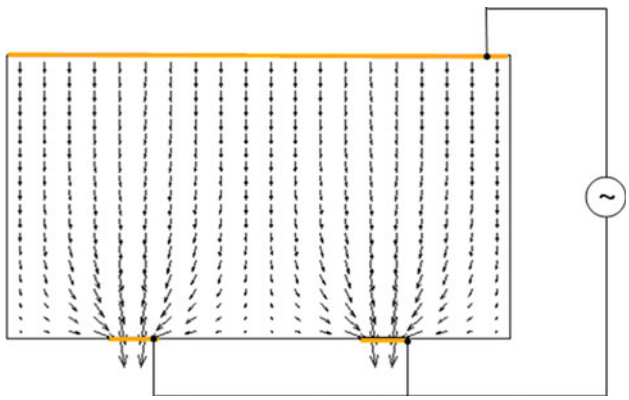

Fig. 8 Normal field generator of the microfluidic electroporation devices depicted in Fig. 7 (Lim et al. 2009)

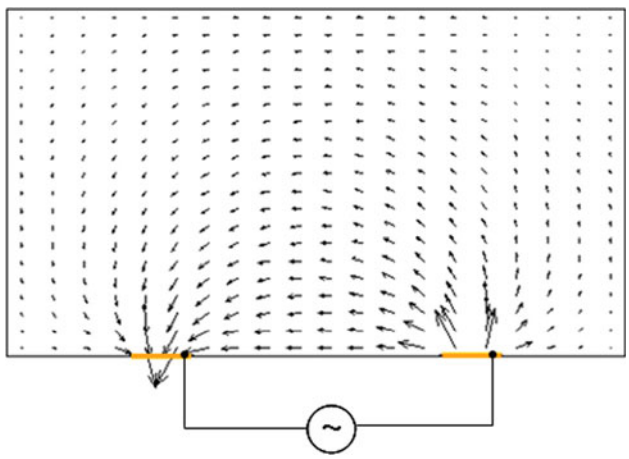

Fig. 9 Co-planar field generator of the microfluidic electroporation devices depicted in Fig. 7 (Lim et al. 2009)

can be trapped by the dielectrophoresis. In this way, the separation process can be carried out continuously.

5.2 Microfluidic electroporation devices for cell transfection (reversible electroporation)

Cell transfection is the most important application of microfluidic electroporation. Cell viability and transfection rate are the two most important indices that are usually used to compare the efficiency of these electroporation devices. Cells must remain viable after transfection, so the electroporation process must be reversible. In comparison with cell lysis, cell transfection usually takes place by lower applied electric field. Tables 1, 2, and 3 show the technical, biological, and electrical properties of these microfluidic devices. Electroporation and cell properties of the different transfection microdevices are summarized in Table 4. In the following, the reported experimental studies of microfluidic cell electroporation–transfection are reviewed in several groups.

5.2.1 Cell trapping-based methods

One of the leading studies using a trapping section in electroporation to fix the cells in the predefined position was suggested by Khine et al. (2005a, b). The manufacturing method of such a trapping section was proposed by Suzuki et al. (2007). Figure 10 depicts this electroporative system. At the center of the system there is one circulation chamber that is connected to many microchannels in radial direction. The two main channels (wider channels) are used as the cell input and output. The other narrower microchannels are utilized as the trapping sections to fixe the cells between the electrodes. The width of these trapping channels is 3.1 μm that is approximately one-third of the cell diameter. Using an external syringe connected to the

Table 4 Electroporation and cell property of the different transfection electroporation microdevices

References	Cell type	Inserted molecule	Optimum state			Single or multi cell	Moving or stationary
			Electrical parameter	Transfected rate (%)	Cell viability (%)		
Wang et al. (2006a)	CHO	SYTOX Green	500 V	56[a]	–	Single	Moving
Wang et al. (2008)	CHO	SYTOX green, PEGFP-C1	800 Vcm^{-1} 1.1 ms	80	–	Multi	Moving
Kim et al. (2007)	K569	GFP	7 V	20	95	Single	Moving
			20 V	70	50		
Khine (2005a, b)	HeLa cell	Trypan blue	–	–	–	Single	Stationary
Valero et al. (2008)	C2C12 cells MSCs	PI, EGFP, ERK1	–	75	~100	Single	Stationary
Wang et al. (2007)	CHO	DNA Dye SYTOX	279 Vcm^{-1} 30 ms	51	70	Multi	Stationary
Fei et al. (2007)	NIH 3T3	GFP and SEAP	35 Vcm^{-1}	~40	~90	Multi	Stationary
Suzuki et al. (2007)	HeLa cell	CFP-improtinβ	–	–	–	Multi	Stationary
Khine et al. (2007)	HeLa cell	Calcein and orange green dextran	–	–	–	Single	Stationary
Luo et al. (2006)	Yeast cells	Fluorescein	–	–	–	Single	Moving
Zhan et al. (2009)	CHO	EGFP	5.8 V	11	–	Single	Moving
			4.7 V	–	68		
			7.1 V	–	14		
Huang Rubinsky (2003)	ND-1 cell line	YOYO-1, EGFP green	–	100	–	Single	Stationary
Shin et al. (2004)	SK-OV-3	PI dye, EGFP green	–	–	–	Multi	Moving
Vassanelli et al. (2008)	CHO	LY	–	–	−50	Single	Stationary
		TB	1.7 V	100			
		ODN	1.7 V	100			
(Lee et al. (2006)	Vesicle	–	1.7 V	100	–	Single	Stationary
Valley et al. (2009a)	HeLa cell	PI Dye	1.5 $kVcm^{-1}$	100	100	Single	Stationary
Zhu et al. (2010)	Yeast cells		1.5 V	70	85	Single	Moving

GFP green fluorescent protein greens, *PI dye* propidium iodide dye

[a] At optimum condition, 56% of transfected cells remain viable

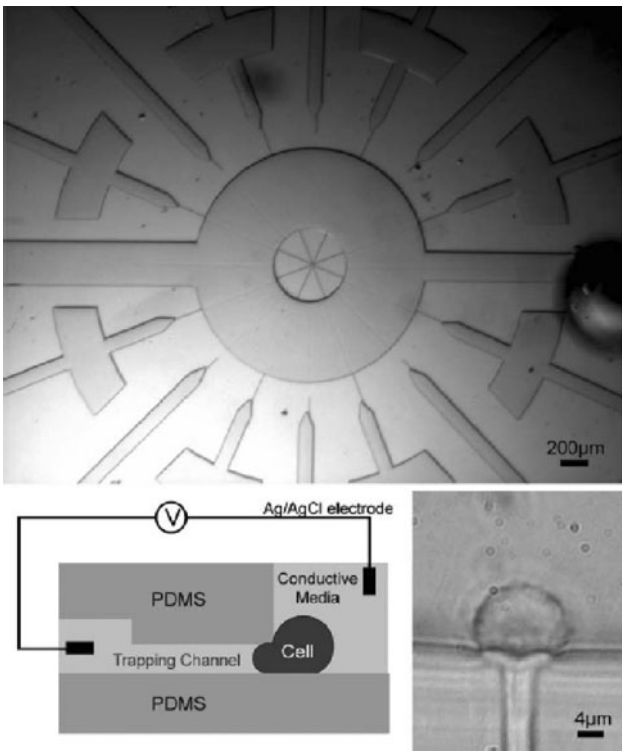

Fig. 10 The image of the microfluidic cell transfection system proposed by Khine et al. (2005a, b). The schematic diagram of the trapping section and the place of electrodes are shown. In this system, the negative pressure is induced to trap and fixe the cell

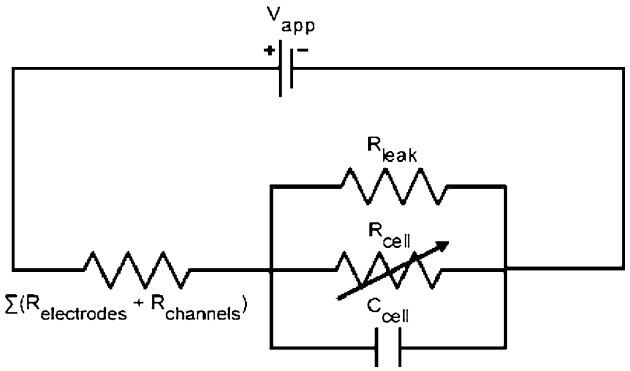

Fig. 11 Electrical circuit model of the cell and chip in electroporation devices of Fig. 10 (Khine et al. 2005a, b)

trapping channels, 2 psi negative pressure is applied to trap the cells between the two electrodes hydrodynamically. One of the electrodes is connected to the main channel, while the other is connected to the small channels (see Fig. 10).

In this system, the happening of the electroporation can be predicted by measuring the electrical parameters. Figure 11 shows the electrical circuit of this system. The cell is modeled as the parallel combination of variable resistances and a capacitor. There is also R_{leak} in parallel with the cell which is because of the leakage around the cell. This parallel part is in series with the electrical resistance due to the microchannels and electrodes. In this system, the trapped cell acts as a high resistance section which can be assumed as two in-series resistances due to the membrane inside and outside the trapping channel. Their images show that the cross section area of the membrane outside the trapping channel is 80 times bigger than the membrane inside the channels which means that the electrical resistance of inside membrane is 80 times bigger than the outside part (electrical resistance is inversely proportional to the surface area). This difference between the electrical resistances focuses the applied voltage over the inside membrane and generates the high electrical field required for electroporation in this part. According to the Ohmic law, voltage and electrical current in the system can be related by electrical resistance $V = IR$. Therefore, for constant voltage, changing in the electrical resistance can result in the electrical current variation. Disrupture in the membrane due to the electroporation can dramatically decrease the electrical resistance in the system which results in the sharp increase in the electrical current. Thus, by recording the electrical current, occurrence of the electroporation can be acknowledged. Using this method, the authors could reversibly electroporate the HeLa cells and the dye can be transfected to the cells by applying 0.76 ± 0.095 V pulse with duration 6.5 ms.

The main issue that may affect the efficiency of the proposed method is the effects of cell deformation on electroporation. In the article, it is indicated that although for short pulses (50 ms) the membrane breakdown was dependent on tension in the membrane; at longer pulses (50–100 ms) the voltage required for the membrane breakdown was tension-independent. By considering the pulse duration of this study (6.5 ms) further investigation must be pursued to study the effect of the generated shear tension on the membrane breakdown.

Another study that used cell trapping to fix cell in transfection process was performed by Ionescu-Zanetti et al. (2008). Figure 12 shows the image of the system used in this study. They suggested using the electrophoresis effect in pre- and post-processing steps of the system proposed by Khine et al. (2005a, b) to decrease the required time of the process. The main idea of the system is shown in Fig. 13. After trapping the cells, the electric field of 0–300 mV is applied to the trapping channels to electrophoretically pre-concentrate the dye near the cell membrane (Fig. 13a). This electric field is considerably lower than the electroporation threshold (0.5–2 V). After preconcentrating, the cells can be electroporated by applying a large amplitude square wave (5–30 ms) while during the resealing period dyes can be loaded into the cells by

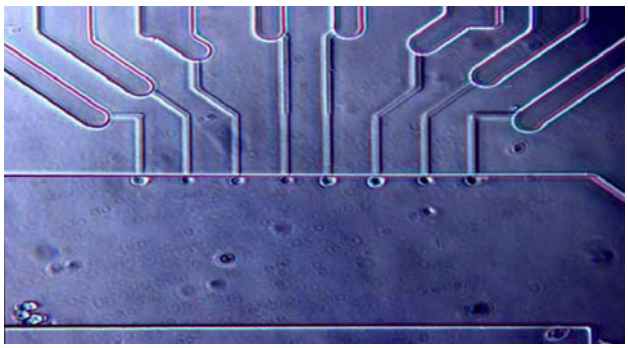

Fig. 12 The Layout of the mechanism suggested by Ionescu-Zanetti et al. (2008)

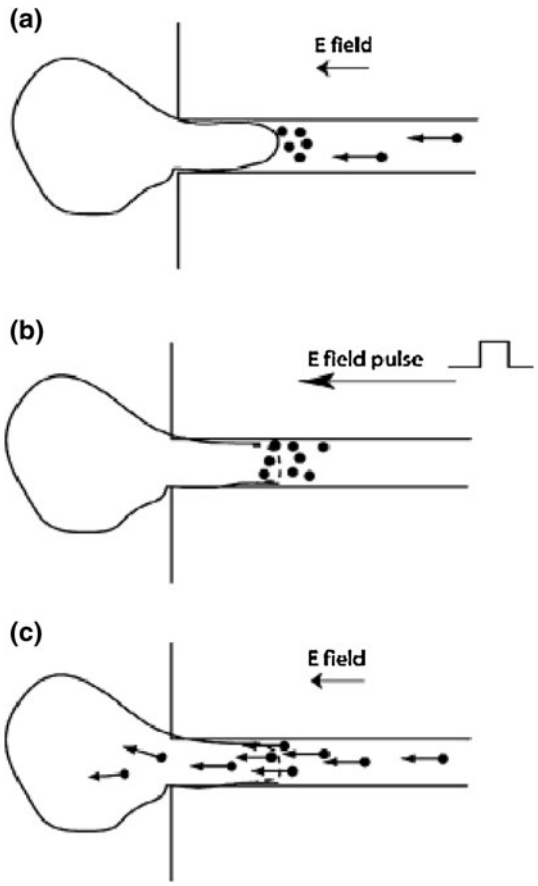

Fig. 13 The schematic steps of the electrophoresis-based electroporation device suggested by Ionescu-Zanetti et al. (2008). **a** Preconcentrate, **b** membrane electroporation, **c** apply electrophoretic driving force

electrophoresis mechanism and by applying the low electric field (for example 200 mV) in the system. Using this method, the required time for loading the dyes into the cell was reduced substantially. For example, Calcein could be transferred into the cell within 3 s, which took 16 s by diffusion alone. They also could load OGD into the cells within 40 s while this time is around 30 min without using electrophoresis effect.

Using their proposed method (Khine et al. 2005a, b, (2007) designed an innovative feedback control system for reversibly electroporate the trapped cells. This system is based on the measurement and monitoring the electrical resistance of the system. As discussed above, by performing the electroporation, the electrical resistance of the system is reduced substantially. In this study, using the mechanism suggested by Cristian Ionescu-Zanetti et al. (2008), the cell was trapped. They monitored the membrane-resistance before, during, and after the electroporation to predict the electroporation happening and to monitor the membrane resealing after electroporation. In order to find the optimum electroporation condition, for various pulse durations (5, 10, 30, and 60 ms), a voltage ranging from 0 to 1 V was applied to the system with the increment of 0.1 V. As the electroporation happened, the sharp change in the electrical current appeared due to the reduction in electrical resistance. Using this method, occurrence of the electroporation can be detected easily. The control program could stop the voltage increasing to avoid further disrupture in cell membrane and significantly decrease the required resealing time for the membrane. After detecting the electroporation, a low-voltage (20 mV) was applied to the system to monitor the resealing kinetic of the cell. The resealing is complete when the electrical resistance recovers to its initial value. Using the feedback control suggested in this study, the reselling time can be reduced significantly; also one specific cell can be reversibly electroporated repeatedly many times. Their results proved the fact that a shorter pulse width, higher voltages is required for electroporation. Shorter pulse width also results in the better membrane resealing. However, there is one problem associates with this method. Although using this method the cell can reseal gently, it may not be enough time for dyes to transfect to the cell. To overcome this problem, the authors suggested using a preconcentration method (Cristian Ionescu-Zanetti et al. 2008).

Another innovative microfluidic device for transfection was proposed by Valero et al. 2008). Figure 14 shows the images of this system. As it can be seen, the system has two main parallel channels (with the width of 50 and 20 μm, respectively) that are connected to each other by nine channels (with the width of 4 μm). These connecting channels serve as the trapping sections to fix the cells in the electroporative zone between two electrodes. Each pairs of microelectrodes oriented at the opening of the trapping channels so that the electric field is focused on the trapped cells. The performance of each microelectrode is independent of the others. Hence, the cells that are not trapped or trapped at the neighbor channels may not be affected in

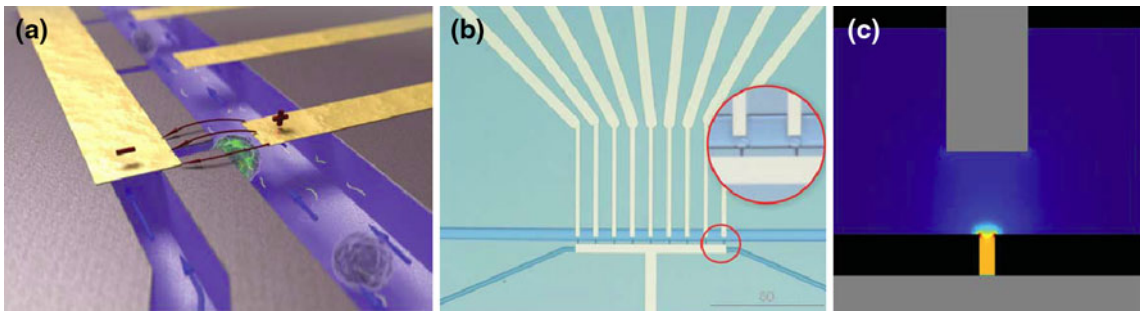

Fig. 14 A single cell electroporation and gene transfection microfluidic device manufactured by Silicon and glass **a** 3D scheme of trapped cells; **b** microfluidic chip picture, zoom-in on trapped single cells; **c** electric field distribution at the trapping sites. Here, a voltage of 1 V yields electric field strength of 0.57 kV/cm (Valero et al. 2008)

the electroporation process of each individual cell. The cells and reagents flow through the upper main channel while the lower main channel is for producing the negative pressure to trap the cells at the opening of the connecting channels. The transfection process includes three main steps. First, the cell samples flowed along the upper channel, meanwhile the lower channel was creating a negative pressure (via a pump, 1–2 psi) to trap the cells at the opening of the trapping channels. After that, the pump was turned off and the DNAs were inserted into the upper channel to transfect to the cells. After 10-min incubating period, 1-V electric pulse with the duration of 6 ms was applied by the microelectrodes to generate the 0.67-kV/cm electric field to transfer the DNAs across the cell membrane. Using this method, they could perform transfection on the C2C12 and MSCs cells by applying a potential of 2 V for at least 6 ms. Their results show that the average transfection rate of their study is $\sim$70% while they have a perfect cell viability ($\sim$100%).

5.2.2 *Membrane sandwich-based microfluidic electroporation*

In a series of articles, Fei et al. (2007, 2010) proposed the membrane sandwich technique (MSE) for cell electroporation. This method suggested immobilizing and sandwich the cells between two polyethyleneterefthalate (PET) membranes to improve the cell transfection and viability. Figure 15 shows the schematic of this system. The system consists of two crossing channels. One channel is located at the top and the other at the bottom of the system. One cuvette was placed at the intersection of the channels as an electroporation section. Figure 15b shows the connection between the channels and the DNA migration path.

The cells are sandwiched between the two membranes. A 3-mm-diameter PET membrane with an average pore size of 400 nm was used as the support for cells. This membrane was fixed at the cuvette by a sealing tape. After that, the suspended cells (NIH 3T3) was loaded onto the supporting membrane and trapped on the supporting membrane by applying the 3-kPa vacuum pressure. Another 3-mm-diameter PET membrane with 3-μm pore sizes was added at the top of the system. The distance between the membranes is 10 μm. The electrodes located at the inlet and the outlet reservoirs (see Fig. 15b). The DNA was loaded to the cathode reservoir. The electrodes have two tasks. First, 300 pulses with the duration of 5-ms and 100-Hz frequency were applied to generate the external electric field of 3.5 V/cm. This external electric field caused electrophoresis force to move the DNAs from the cathode reservoir to the cell culture medium at the center of the system. After that, five pulses with 500-ms duration and

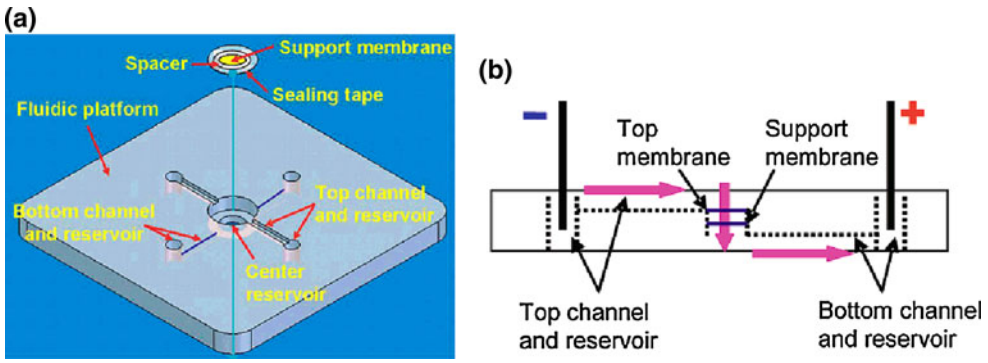

Fig. 15 Schematic diagram of the membrane sandwich electroporation (MSE) technique (Fei et al. 2007)

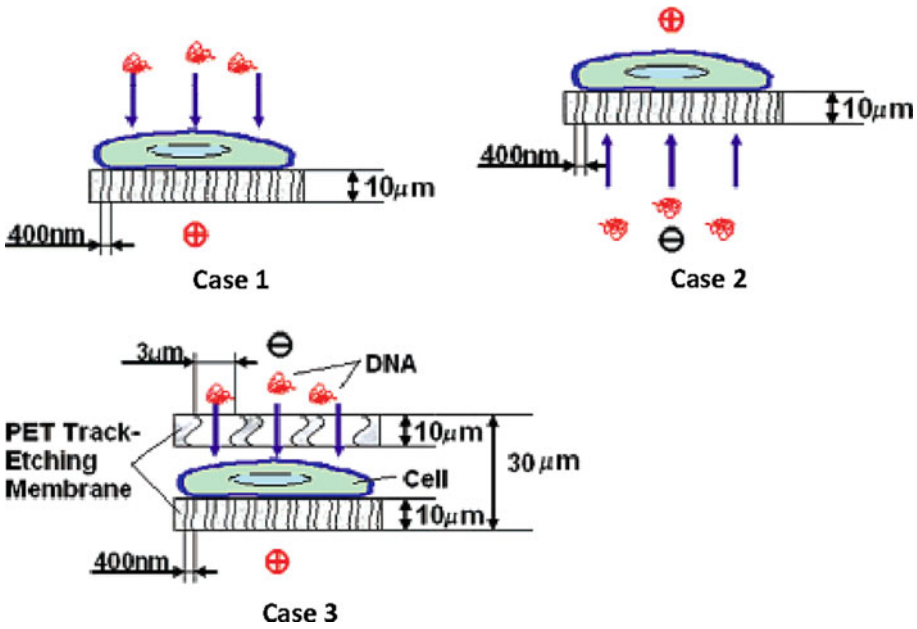

Fig. 16 The orientation of cells and DNAs with respect to each other in three parts of the experiments accomplished by Fei et al. 2007)

1-Hz frequency were applied to generate the 35 V/cm electric field to perform the electroporation. This system was utilized to transfect the plasmid GFP into the NIH 3T3. Two different experiments were performed and the results were compared with the conventional electroporation from the literature (see Fig. 16). The substantial improvement in the cell transfection was recorded compared to the conventional cell electroporation techniques. Using this method, the cell viability and transfected rates are 90 and 40%, respectively.

In fact, the sandwich membranes prevent the diffusion of the DNA molecules from the membrane surface. After applying the external electric field, membrane becomes negatively charged. This may repel the negative DNA molecules. The two negatively charged membranes trap the DNAs in the small volume near the cells and concentrate the DNAs near the cell membrane. This may result in the increase in the DNA transfection to the cell.

5.2.3 Polyelectrolytic salt bridges

Utilizing ionic bridge has been suggested in many microfluidics applications (Park et al. 2009). Kim et al. (2007) suggested using ionic conductivity of polyelectrolytic gel electrodes for electric field concentration and cell electroporation. The microfluidic electroporator device was designed to work under a continuous low DC voltage (7–15 V). Figure 17 shows the schematic diagram of this mechanism. The two electrodes are placed in the hypertonic solution. A pair of pDADMAC plugs on both sides of the microchannel separates the cell suspension and hypertonic solution. The pDADMAC plugs have a good ionic conductivity. The chip was designed to have low

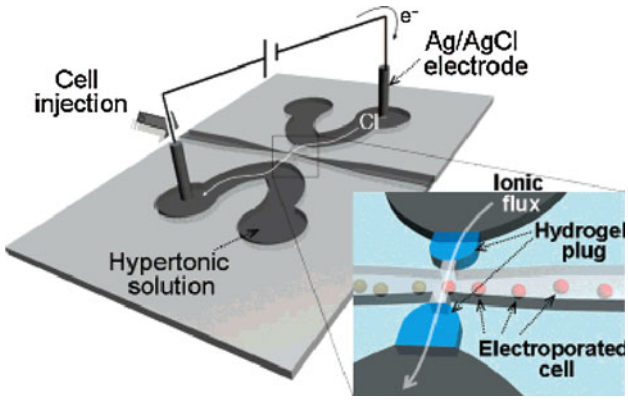

Fig. 17 The schematic of the microelectroporation chip that use ionic conductivity of polyelectrolytic gel electrodes for electric field concentration. Cells experience an electric field gradient by passing through the region between the salt bridges (Kim et al. 2007)

impedance so that a large portion of the potential difference is applied at the cell solution. In the article, the pDADMAC plugs and the hypertonic solution have the identical ionic conductivity (equal to 16 Sm^{-1}), while the ionic conductivity of the cell media solution is ten times more resistive. This difference leads to concentrate the electric field on the cells. Using this method, they could generate an electric field of 0.9 kV/cm over the microchannel with the input voltage of only 10 V. This value of electric field is sufficient for performing electroporation of K562 human chronic leukemia cell.

In this study, the electroporation efficiency is defined as the number of live permeated cells divided by the number of live cells after electroporation. The viability is defined as the ratio of live cells to dead cells. For a constant cell velocity at 3.2 cm/s, they investigated the effects of input

voltage on electroporation efficiency and cell viability. Their results show that increasing the input voltage from 7 to 20 V results in increase of the efficiency from 20 to 70%; however, it also brings about the cell membrane damage that decreases the cell viability from 95 to 50%. One important parameter in cell electroporation is the pulse duration. This article also includes some results of the effect of pulse duration on electroporation. By increasing the cell velocity from 1 to 8 cm/s (which results in decreasing the pulse duration), the cell viability is increased from 70 to 95% while the electroporation efficiency dramatically decreases from 75 to 15% (input voltage is constant and equal to 15 V).

The method of this study has some advantages: there is no bubble generation, heating shock, and chemical contamination associated with this method. The main reason for these positive points is that the electrodes are placed in the buffer solutions that are completely isolated from the electroporative section and cells. However, there is one limitation associated with the method. The pDADMAC plug has the tendency to swell as it absorbs water. This plug expansion can be high enough to block the channel.

5.2.4 *Using mechanical valve*

Using mechanical valves in microfluidic electroporation devices was presented by Wang et al. (2007). The scheme of the experimental system of this study is shown in Fig. 18. The system consists of fluidic channel (black one), control channel (gray one), DC power supply, solenoid valve, and control unit. There is a PDMS membrane between the fluidic and control channels. Constant DC voltage is applied to the system by power supply. The valve is located in the vertical fluidic channel (channel 1), while the horizontal fluidic channel 2 is used as the cell culture channel. If the electrical pulse with proper duration and intensity is applied in fluidic channel 2, the electroporation can be performed on the cells in this channel. The electric pulse was generated by the control channel that turns on and off a DC electric field by physically

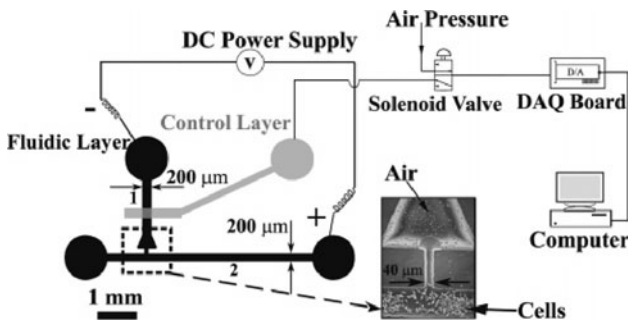

Fig. 18 The schematic diagram of the electroporation microfluidic device that use mechanical valve for cell transfection (Wang 2007)

connecting and separating the ionic buffer. The solenoid valve controls the operation of the control channel (gray one). The roll of the valve is to pressurize the PDMS membrane between the fluidic and control channels to block the fluidic channel 2, and hence the electrical current in fluidic channel 2. If the valve operates in a close–open–close sequence, the electrical pulse can be generated in the fluidic channel 2 to perform the electroporation.

Several parameters can affect the performance of this system: control channel width, actuation pressure (inserted by Solenoid valve), valve opening time, and applied constant DC voltage. The authors tested different values of these operating parameters and finally used the control channel with a width of 300 μm and applied 40-psi pressure for 30-ms opening time. Using these parameters, they could reversibly electroporate the CHO cells and insert the SYTOX green into the cell. At optimum condition (279 Vcm^{-1} electric field with 30-ms duration), the transfection rate and cell viability are 51 and 70%, respectively.

This system is based on the insulating nature of the PDMS valve (membrane). It was indicated in the article that long time contact between the PDMS and culture media can weaken the PDMS insulating property; therefore, they used a triangular structure between the fluidic channels 1 and 2 to completely separate the culture media (in fluidic channel 2) and the PDMS valve (fluidic channel 1).

The main advantage of this device is its ability to electroporate the cells in the culture media and electroporate the adherent cells. The electroporation of the cells that adhere to the substance is desired because of the minimum defection to the cell culture. There are also some disadvantages of this method: First, the moving part and the limitation associate with it such as fatigue, vibration and so on. In addition, this system is based on the insulating property of PDMS valve that can be weaken over time. Furthermore, the manufacturing process of this system seems not easy. Finally, the applied voltage to this system (200–1000 V) is considerably higher than the applied voltage (up to 100 times) in the other proposed electroporative systems. This high voltage can cause bubble generation, significant Joule heating effect, and also requires more safety measures.

5.2.5 *Single cell electroporation microarray*

Vassanelli et al. (2008) developed a new chip to conduct electroporation of single cells attached to the growing surface. Figure 19 shows the schematic of this chip. This chip has an array of 60 circular cell-size microelectrodes. The microelectrodes are connected to the external circuit by a metal line that is covered by a 200 nm layer of

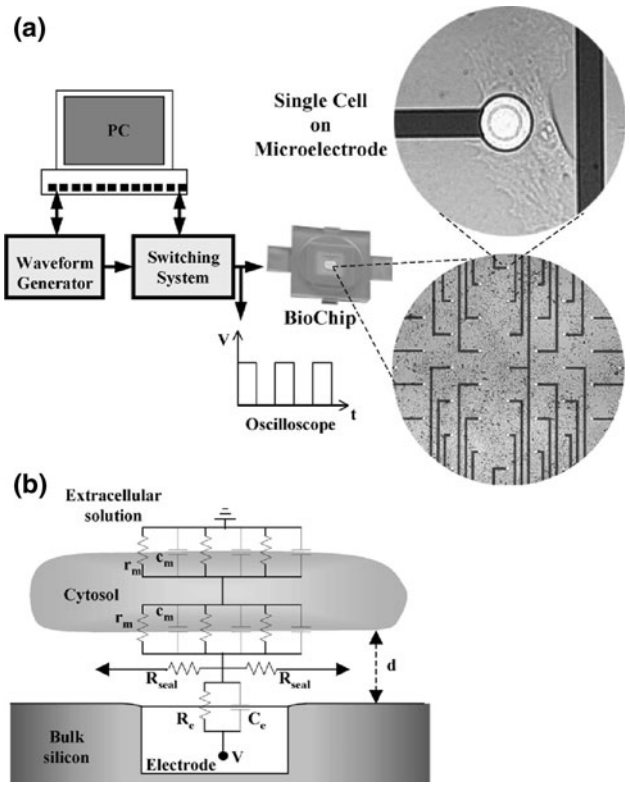

Fig. 19 **a** Schematics of a BioChip device and its control system used microarray for single-cell electroporation. The control system driven by a personal computer. **b** Equivalent electrical model of the coupling between cell and chip (not to scale) (Vassanelli et al. 2008)

amorphous silicon nitride (Si_3N_4) to be insulated from the extracellular electrolyte. The electric potential can be applied to the cells via the circular gold layer at the ends of electrodes. The diameter of these free surfaces varies from 15 to 50 μm, while the distance between microelectrodes was either 150 or 300 μm. The duration and the intensity of the applied voltage at each microelectrode can be controlled individually. In this way, each target cell can be directly electroporated in situ. There is no need for cell detachment and harvesting that can be harmful to the cell structure. Instead, the pre-programmed control system activates the microelectrodes near the target cell to electroporate it. The time of electroporating each cell can also be different from the others. This may lead to the sequence electroporation of single cells. The cells may be electroporated many times while the different molecules are delivered to the cell.

Using this chip, the different molecules (LY, TB abd 24 nt ODN) were inserted into the CHO cell by performing the reversible electroporation. The train of five 10-ms pulses were applied to the target cells. Below the applied voltage of 0.9 V, no uptake was recorded. Increasing the voltage from 0.9 to 1.3 V leads to the increase transfection of LY and TB. Above 1.3 V, ODN was also started to enter to the cell. At 1.7-V applied voltage, the uptake efficiency of ODN was about 70%, while 100% efficiency was recorded for LY and TB. In comparison with the other methods, there are many advantages associated with this one. First, the required voltage is relatively low. The transfection could be performed by applying only 0.9–1.7 V DC voltage. There is no need to detach and harvest the target cells. There is no restriction on the time for electroporating cells in one specific culture medium. Cells can be electroporated independently from the others. The sequence electroporating of one specific cell could also be performed by this method. However, it was claimed in the article that this technique cannot be applied to the cells in a tissue.

5.2.6 Droplet microfluidic electroporation

The idea of using microfluidic droplet electroporative devices was first suggested by Luo et al. (2006). The device can electroporate the yeast cells encapsulated in the droplets. Following this study, Brouze et al. (2009) presented a droplet-based microfluidic technology that shows the feasibility of high-throughput screening of single mammalian cells. They could encapsulate the single cells and reagents in the independent aqueous microdroplets and also manipulate and monitor the droplets. A critical study on the microfluidic droplet electroporation was conducted by Zhan et al. (2009). The schematic diagram of this electroporative device is shown in Fig. 20. The chip has two inlets and one outlet. The inlets are connected to two reservoirs to supply non-conductive oil and the mixture of cells and ionic conductive buffer solution, respectively. First, the cells were encapsulated in the aqueous droplets flowing in the oil. In the downstream, the flow went through a pair of microelectrodes that apply a constant DC voltage to the system. Because the oil is non-conductive, the cell experienced a transient electric pulse whose shape and duration depend on the velocity and dimensions of the droplet, electrical parameters of the system, distance between the electrodes, and location of the encapsulated cell in the droplet (see Fig. 20). In this study, the velocity and dimensions of the droplets and also the distance between the electrodes are 1.38–8.86 m/min, 60–386 μm in the length, and ~20 μm, respectively. The main drawback of the droplet microfluidic electroporation is the effect of oil on cell viability. This study recorded 11% cell death due to the contact between the cells and the oil droplet. The percentage of viable cells dropped from 68 to 14% by increasing the applied voltage from 4.7 to 7.1 V. Using this method, a plasmid vector coding EGFP could be transfected into CHO cells with the applied voltage of 5.8 V and the electroporation zone transit time of 1.8 ms.

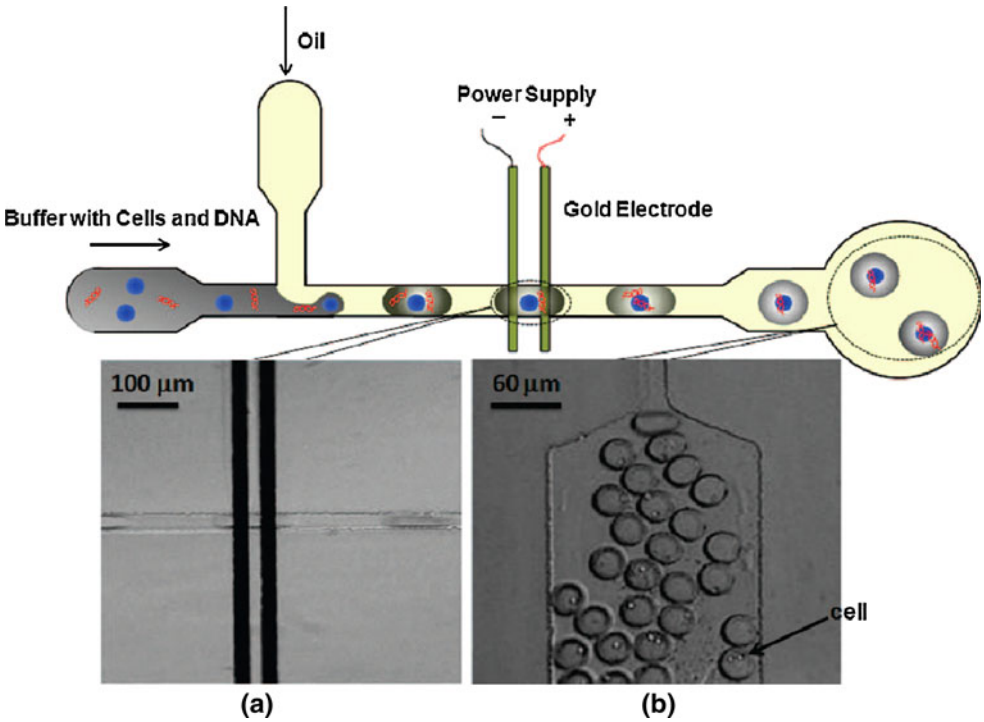

Fig. 20 Schematic diagram of the droplet-based microfluidic electroporation. **a**, **b** are the images of the droplets at different sections of the system. **a** The electroporation section that the droplets rapidly flow through the two microelectrodes on the substrate (each electrode was 25-µm wide, and the distance between the two electrodes was 20 µm). **b** Exit reservoir of the system where the droplets with encapsulated cells collected there after electroporation (Zhan et al. 2009)

5.2.7 *Optofluidic-based microfluidic electroporation device*

Recent studies proposed using optofluidic technology in biology (Brennan et al. 2009) and cell study (Sott et al. 2008; Lin and Leea 2009). In the series of articles, Valley et al. (2009a, b) proposed using a photosensitive surface and patterned light to create virtual electrodes to manipulate and electroporate single cells. The main advantage of this method is the ability to perform in situ electroporation. Figure 21 schematically illustrates the device. It consists of two glass substrates coated with a layer of the transparent conductor indium tin oxide (ITO). The bottom substrate is coated with a photosensitive film (a-Si:H). A layer of lithographically patterned SU-8 defines the channel geometry and serves as the spacer between the top and bottom substrates. The space between the two substrates is filled with a solution containing the cells of interest. The two ITO layers were used to apply an AC voltage to the system. In the absence of light, most of the electric field is concentrated across the highly resistive photoconductive layer. However, upon illumination, the resistance of the photoconductive layer (in the illuminated areas) decreases by many orders of magnitude due to creation of electron–hole pairs. This causes the majority of the electric field to be applied to the liquid layer wherever the device is illuminated. Therefore, if an object, such as a cell, is illuminated, the electric field will be concentrated on it.

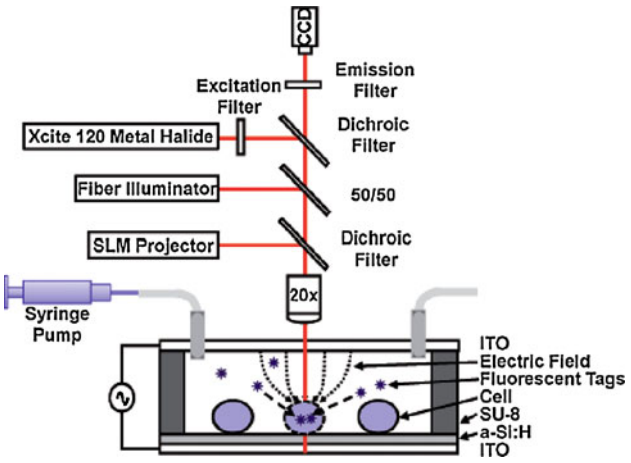

Fig. 21 Cross section of the optofluidic-based microfluidic electroporation device. Experimental setup and mechanism of the light-induced electroporation system are demonstrated. The electric field concentrates across the illuminated cells by creating the virtual electrodes near the cell membrane (Valley et al. 2009a)

The optical power density required to operate the device is low (1 W/cm) that can be supplied by a standard projector. Therefore, the simplicity of the supporting equipment is another advantage of this method. They showed that 0.2 kV/cm AC electric field with 100-kHz frequency could produce the required dielectrophoretic force to manipulate and trap the HeLa cells in the predefined positions. By intensifying the electric field to 1.5 kV/cm the cells could be reversibly electroporated. Their results show the high efficiency of the proposed method, the cells could be electroporated individually while the surrounding cells remain intact. Therefore, the single cell electroporation can be performed with very good efficiency.

5.2.8 *Cell transfection in continuous flow in microchannels*

Wang et al. (2006a, b, c) used the electroporation device reported in their previous studies to insert the SYTOX green dye and pEGFD-C1 protein into the CHO cell (see Fig. 4) (Wang et al. 2008). The constant voltage was applied along the channels while electric pulses were generated by the geometric variation of the microchannel. Their results show that the percentage of viable cells is increased up to the field intensity of 500–600 V/cm. For higher field intensities, the pulse duration must be lower than 6 ms in order that the cells become viable. According to their results, if the electrical parameters are tuned properly in the system, increasing the number of narrow sections (and hence the number of pulse and pulse duration) in the microchannel improves transfection efficiency (see Fig. 22). For example, the device with five 700 V/cm pulses and the durations of 0.22 ms has the transfection efficiency of 21.2%, while this efficiency is 14.4% for the device with one 1.1-ms pulse.

In another their study, they showed that the cells started "growing" immediately when electroporation began (Wang et al. 2006b). It may be caused by the difference between the permeability of the ions and larger-molecules (macro-molecules) inside the cell. In this study, the mechanism suggested in their previous studies (Wang et al. 2006a) was used to study the cell swelling and the cell rupture. For the first several hundred milliseconds, the cells were exposed to the electric field of 200–500 V/cm. They used three different buffer solutions with 8-mM Na_2HPO_4, 2-mM KH_2PO_4, sucrose of various concentrations [hypotonic: 125 mM, isotonic: 250 mM, and hypertonic: 375 mM, and pH value of 7.4]. In these solutions, the increase in the cell volume was observed and the swelling rate and the rupture of cell membrane in the real time at single cell level were recorded.

For external electric field of 400 V/cm, Fig. 23 shows the swelling of one CHO cell at different points of

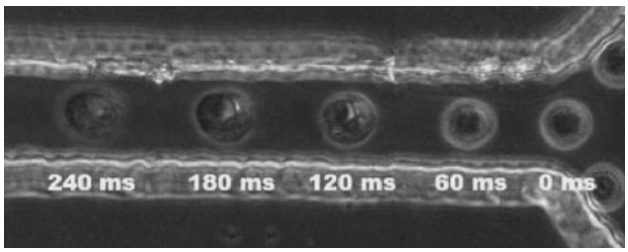

Fig. 23 The time-sequence images of the same CHO cell flowing in the isotonic buffer (10-mM phosphate and 250-mM sucrose; $E2 = 400$ V/cm). The images were captured at a rate of 16 Hz. The velocity of the cell was in the range of 0.1–1 mm/s (Wang et al. 2006b)

electroporation sections of the device and at different time. The cell velocity is 0.1–1 mm/s and the buffer solution is isotonic. This figure shows the cell growth in the presence of electric field. Their results show that the swelling and the membrane rupture occurs more rapidly in hyper- and hypotonic buffers than in isotonic buffer. For example, for the field intensity of 400 V/cm and isotonic buffer solution, there is 128% increase in the average percentile of the cell diameter after 300 ms; while this value is 149 and 145% in the hypotonic and hypertonic buffer solutions, respectively. The results show that the swelling rate is more considerable in hypotonic than hypertonic solution. They assumed that the swelling is because of water influx into the cells when the electropores are open. Based on this assumption, they concluded that the electropore density and size are higher in hyper- and hypotonic solutions. Therefore, hyper- and hypotonic buffer could contribute to the increased delivery of biomolecules into the cells. However, there is another theory for the swelling modeling rather than the water influx that will be explained later.

Using the proposed techniques by Wang et al. (2006a), Geng et al. (2010) delivered genes into CHO cells at high flow rates (up to ~20 ml/min). With the optimal design, ~75% of the viable CHO cells were transfected after the procedure (Schaper et al. 2007). Bao et al. (2010) utilized the electroporation microfluidic device proposed by Wang

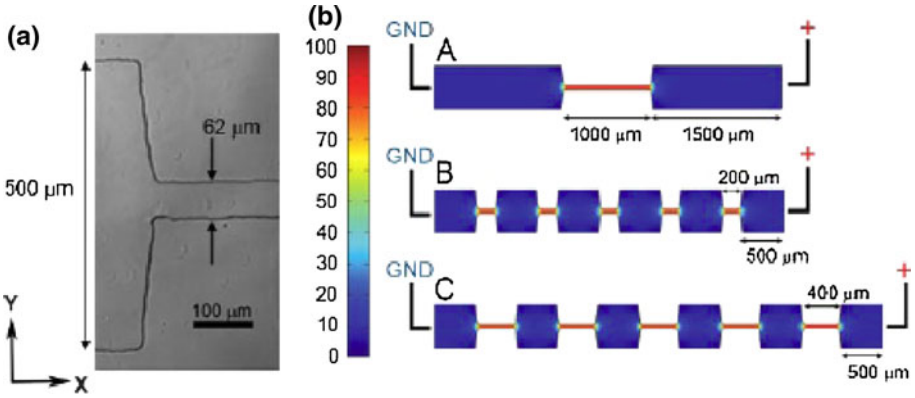

Fig. 22 The field intensity in electroporation microfluidic device that utilize cross-sectional geometric variation to generate electric pulse (Wang 2008)

et al. (2006a) to electroporate blood cells. These cells are circulating tumor cells (CTC), red blood cells (RBC), and white blood cells (WBC). CTC refers to the cells that detached from the primary tumor. They circulate in the blood stream and may settle down at a secondary site and from metastases. Their results show that there is a significant difference in the threshold electric field for the irreversible electroporation of these cells. For example with the pulse duration of 100–300 ms, the irreversible electroporation was occurred at 300–400, 400–500, and 1100–1200 V/cm for M109 tumor cells, white blood cell, and red blood cell, respectively. These differences could lead to the selective electroporation in the stream of blood cells. The difference between the cell diameters is the reason of these different threshold values. For the identical external electric field, the cells with the bigger radius have the higher transmembrane potential and are easier to be electroporated at lower external electrical field.

This article (Bao et al. 2010) also includes some interesting results on the swelling of cells during the electroporation. Using the coherent anti-Stokes Raman scattering (CARS) microscope and fluorescence microscopy tools, they could observe the subcellular changes during the swelling. Their results show that the major part of the swelling is due to nucleolus expansion. According to their results, the nucleus of the cell starts expanding upon applying the external electric field; if the applied electric field is removed, the nucleus will shrink. Under 400 V/cm applied electric field, Fig. 24 shows their captured images in different times. For 400-V/cm external electric field, they also have depicted the separate rates of the nucleus and cytoplasm expansion versus time (see Fig. 25). This

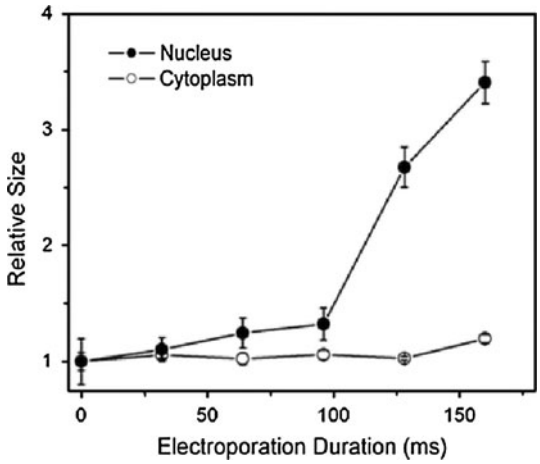

Fig. 25 The relative increase in the size of cytoplasmic and nucleic areas during the swelling. The original size at time 0 is designated as 1 (Bao et al. (2010)

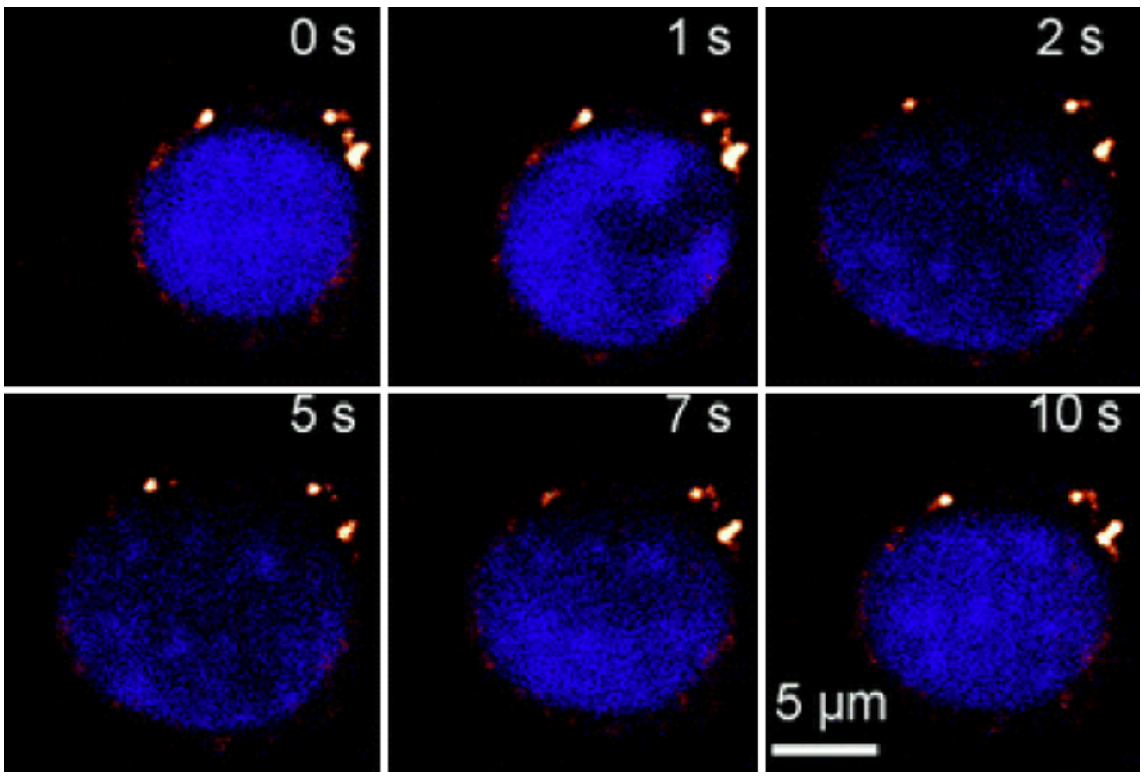

Fig. 24 Nucleus expansion in a M109 cell. The CARS signal and TPEF were utilized to detect the Lipid rich structures and Hoechst 33 342-stained nucleus, respectively. The electric field of 400 V/cm was applied

diagram shows that the cytoplasm approximately remains unchanged during the electroporation. According to their findings, they suggested one of two possible mechanisms (that are potentially mutually exclusive) to be responsible for the cell expansion during electroporation. However, they could not conclude that which one of these two theories is true. First, the expansion is due to solution influx into cells, as suggested in previous studies. However, the influx solution preferably locates in the nucleus (instead of the cytoplasm) after entering through the membrane. Second, the solution influx only accounts for a minor contribution to the expansion. Cells expand mostly due to the nucleus expansion when electroporated.

Zhou and Tilton (2010) studied single cell electroporation in continuous flow field. Figure 26 depicts the schematic diagram of the system. The cellular suspension was injected to the sample channel from its inlet. The KCl solution meanwhile was injected from the channels on both sides. They were driven by the computer-programmed syringe pumps. In the confluent channel of two fluids, the cellular suspension flow was squeezed into a thin laminar layer by the KCl solution flows. A constant DC voltage was applied onto two chlorinated Ag wires punched in the inlets of the KCl channels, to produce a large potential drop on the cellular flow of the central layer. According to Ohm's law, as the conductivity of the KCl solution is much higher than that of the cellular suspension solution, major voltage drop will occur over the central layer of the flow. Because the size of the cellular flow could be changed by varying the speed ratio k of the flows, the width of the central layer could be very small (<20 μm as the velocity ratio $k = 2$). Therefore, a low voltage supply (e.g., around 1.5 V) could generate a high electric field on the narrow cellular layer to accomplish electroporation with a limited pulse duration. At the optimum operating condition, they could successfully transfect the Yeast cells by only applying 1.5 V to the system. In this optimum condition, the cells have 70% viability while the transfection rate is around 85%.

5.3 Microfluidic electroporation in other processes

Many other studies utilized cell electroporation for other applications such as electrofusion (Cao et al. 2008; Schaper et al. 2007), metabolism monitoring (Cheng et al. 2010), localization of Kinases within cells (Wang et al. 2008), and inactivation of *Lactobacillus plantarum* by pulsed electric fields in a microfluidic reactor (Fox et al. 2008). Electrofusion is the method to create hybrid cells by utilizing high-voltage electrical pulses. It consists of three main steps: cell alignment, electroporation, and fusion. A key step in electrofusion is the electroporation of the cells that are desired to be attached to each other. One of the microfluidic systems that are utilized for electrofusion was developed by Cao et al. (2008). Figure 27 schematically shows the system. There are up to 2,376 microelectrodes located on the chip. The electrodes were placed on both sides of channels. The microchip consists of six microchambers with the serpentile microchannels. The depth and width of the channels are 20 and 80 μm, respectively. The distance between the microelectrode pairs on both sides of the microchannels varies from 50 to 100 μm with the increment of 10 μm in each microchamber. In this way, one can also have a better control on the electric field applied to each cell. Using this system, two kinds of cells have been electroporated for electrofusion (animal HEK-293 cells and plant cucumber mesphy II protoplants). The applied

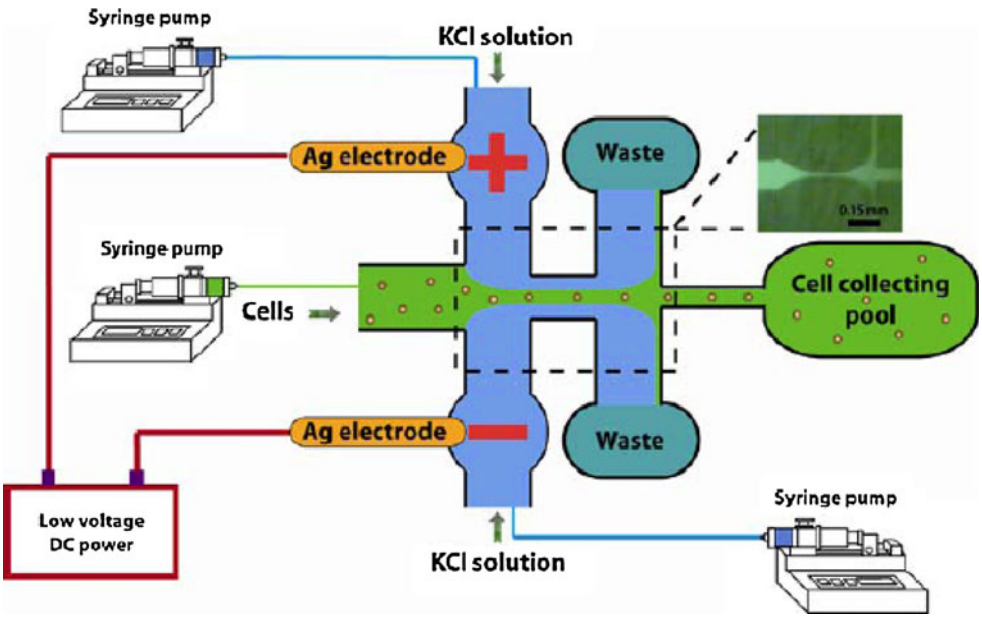

Fig. 26 Schematic of the electroporation chip used hydrodynamic focusing during the electroporation process. By going through the focusing region, cells experience a local electric charge of high density. The figure located at the *upper-right corner* shows the fluorescence images captured during the experiment (Zhu et al. 2010)

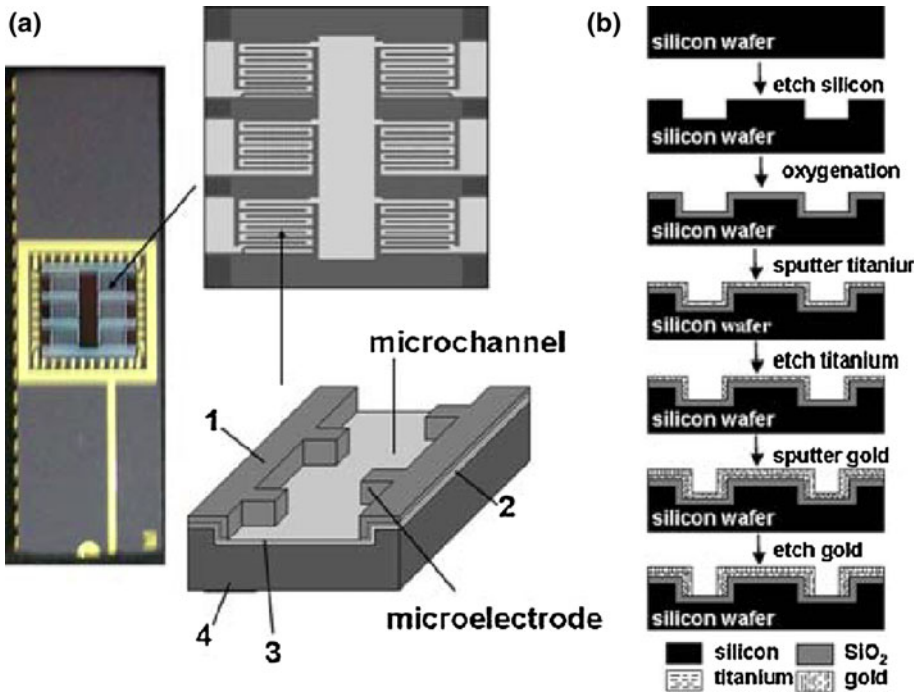

Fig. 27 The schematic diagram and manufacturing process of the Cell-fusion chip. **a** The layout of a cell-fusion microchip, microchannels, microelectrodes on the chip, and the 3D schematic diagram of the system. **b** The manufacturing process of the system. The tagged areas are: (*1*) Au, (*2*) Ti, (*3*) SiO_2, (*4*) Si (Cao et al. 2008)

electrical pulse for electroporation is 3–7 kV/cm with 20–50-μs duration. Considering the distance between the microelectrode pairs (50–100 μm), approximately 20–50 V voltage needs to be applied. Although this is not so high in comparison with the other electroporative microdevices (see Table 1), Joule heating effect and bubble generation may occur and must be considered carefully.

6 Characteristics of the current studies of microfluidic electroporation

6.1 Microfluidic devices for cell transfection

Transfecting rate and cell viability are the two most important parameters for evaluating the performance of each cell transfection process. Along with these parameters, single or multi cell electroporation is the other important parameter. Table 4 summarized these parameters for the reviewed articles of this study. From this table, it is clear that the microfluidic electroporation devices that trap the cells during the electroporation have better cell viability and transfection rate. They could also perform single cell electroporation that is desired in cell biology. For example, in the study done by Valley et al. (2009a), approximately all the cells are transfected and remain viable; or in the study accomplished by Valero et al. (2008), more than 75% of the cells were transfected during the electroporation and approximately all the cells remain viable after electroporation. For systems that perform cell transfection while the cells are in motion, partial cell transfection is usually recorded while the cell viability is also not as high as the trapping cases (Kim et al. 2007; Zhan et al. 2009).

Trapping cells usually were carried out by inducing negative pressure at the trapping channels (Khine et al. 2005a, b) or using dielectrophoretic force (Sedgwick et al. 2008). In the studies that used trapping channel and induced negative pressure, deformation of cell membrane during the trapping process was observed. This may damage the cell membrane structure and be harmful for cell viability. Using dielectrophoresis force for cell trapping may also ruin the cell structure due to the applied electric field. Finding other methods to fix the cells in predefined electroporating sections is preferred. For example, obstacles can be considered to hold the cells in the desired location.

Another important criterion in assessing the performance of reversible electroporation microfluidic devices is the ability of predicting cell permeabilization. If the occurrence of cell electroporation is identified quickly, the applied electrical parameters can be modified to prevent cell death and increase the cell viability (Khine et al. 2007). Especially in the cases of fixed single cell electroporation, this can be done by measurement of electrical current in the system. This is because the incident of cell permeabilization generates the sudden decrease in electrical resistance of the cell membrane; this gives rise to sharp increase in electrical current. Therefore, by monitoring electrical current in the system, the occasion of cell membrane permeabilization can predicted easily (Khine et al. 2005a, b, 2007; Vassanelli et al. 2008). However, no experimental

set-up has been reported yet that can predict the internalization of dye to the cell during the reversible cell electroporation. The occurence of cell internalization is usually recorded using microscope to watch the process or capture the pictures.

6.2 Electrodes

The characteristics of the electrodes of the reviewed articles are summarized in Table 1. To perform the electroporation, high electric field is required. Electrodes usually are positioned in two different manners: very close or far from each other. In the first approach (Lu et al. 2005; Ikeda et al. 2007; Cao et al. 2008; Sedgwick et al. 2008; Luo et al. 2006; Zhan et al. 2009), the electrodes were placed with 10–100 μm, and the cells were placed in the gap between the two electrodes. Using this method, the presence of electric field in the system can be restricted to the local area. In can eliminate (or at least decrease) many drawbacks which are associated with the presence of electric field in the overall system such as Joule heating, bubble generation, extreme pH condition, and swelling of the cells. However, depending on the pulse duration and the intensity these side effects may be still present in the regions near the electrodes. Furthermore, the electrodes can be the source of many contaminations in the system that may be harmful for the cell viability. By considering these limitations, it may be concluded that this method may not be suitable for the cases that high intensity and/or long duration of electric field is required.

In the other approach, the electrodes are placed far from each other (Wang 2006a, b, 2008; Bao et al. 2008, 2010; Kim et al. 2007; Khine et al. 2005a, b, 2007; Valero et al. 2008). The applied voltage by the electrodes usually generates the electric field below the electroporation threshold. This electric field is then intensified to the higher values above the electroporation threshold in some specific parts of the system (the electroporative sections) by some mechanisms such as geometric variation or placing the cell in a high electric resistance medium. Decreasing the cross-section area of the microchannel will result in electric field intensification in that region. Moving cells through this high voltage region will be electroporated. The duration of electric pulse is determined by the cell velocity and the length of the narrower section of the microchannel. If the cell will be put in a medium that its electrical resistance is substantially lower that the cell's electrical resistance, the applied voltage can be focused on the cell. This method has some positive and negative aspects. The presence of low intensity electric field in the system can be utilized for many pre- and post-processing steps such as cell handling and cell separation. Because there is a weak electric field in most parts of the system, Joule heating, bubble generation, and electrolysis may not be so important. However, the previous studies show that the effect of cell swelling can become important in the system. Cells start growing when they are exposed to the external electric field. Continuous electric field will result in the non-stop growth of the cell. This may have some effects on the cell electroporation. For example, due to the cell expansion, the cell is electroporated at a lower applied electric field; the larger size of the growing cells may block the microchannels.

In order to decrease and prevent bubble generation and extreme pH condition near the electrodes, usage of AC field instead of DC field was suggested. To eliminate the effects of electrode contamination on the electroporated cells, the isolation of the electroporated media from the electrodes was proposed (Lee and Tai 1999; Kim et al. 2007). For example, Kim et al. (2007) proposed using two salt bridges with the ionic conductivity equal to the buffer solution to separate the cell culture from the electrodes. Because of the hydrophilic nature of the salt bridge, it may start expanding which may results in the microchannel blockage. Choosing the optimized designed parameters for the salt bridge can decrease the effect of this problem.

6.3 Cell types

Studies before 2005 usually used the cells that are relatively large in size such as animal cells, yeast, and plant cells. The transmembrane potential depends linearly on the cell diameter. Therefore, the larger cells can be electroporated by relatively lower applied voltage. The detection of the larger cells is also easier (Fox et al. 2006). To have better treatments on the human diseases, studies of the human cells are essential. In the recent studies, some researchers worked on the electroporation of human cells, such as HT-29 cell, RBC, EBC, M109 tumor cell, K569, HeLa cell, and HEK 239 (Lu et al. 2005; Bao et al. 2010; Kim et al. 2007; Khine et al. 2005a, b; Fei et al. 2007; Suzuki et al. 2007; Cao et al. 2008; Brouzes et al. 2009) and also the cells with the smaller dimensions such as *E. coli* cells (Wang et al. 2006c; Valero et al. 2008). While the reversible electroporation and transfection of the cells are important, the precise analysis on the intercellular contents of the cells via cell lysis is also critical.

6.4 Other factors in electroporation

In many applications, cell position and orientation must be monitored carefully. For example, in electrofusion, the two distinguished cells must be aligned to each other before performing electroporation. In the cell lysis, cells must be restricted in the specific volume that the released materials can be collected easily. As summarized in Table 2, during the electroporation, cells can be static or moving. In the

electroporation of moving cells, the cell velocity and the length of the electroporated sections play important roles on the electroporation quality. This is because that the pulse duration can be adjusted by tuning these two parameters. In the static cell devices, cells are usually trapped by inducing the negative pressure or by applying the dielectrophoretic forces. The advantages of static cell electroporation include the ability of monitoring the electroporation process and resealing process, performing ion pre-concentration near the cell membrane, and using the electrophoretic forces to hustle the transfecting of the molecules into the cells (in the post-processing step). However, the effects of trapping forces (dielectrophoresis or hydrostatic pressure) on the cells must be considered carefully. They may cause shear stress in the cell membrane and have a permanent distorting effect on the membrane structure. This may lead to the cell membrane disrupture.

The other important factor in electroporation is the quantity of cells that are electroporated. Bulk electroporation usually electroporates thousands of cells simultaneously. High voltages are usually applied in bulk electroporation; this is usually associated with the excessive Joule heating, bubble generation, electrode contamination, uncontrolled, and nonhomogeneous electric field across the different cells, and low viability and low electroporation efficiency. Above all, the obtained results of the bulk electroporation represent the average response of all cells to the applied electric field while the individual reaction of cells to the applied electric field may be substantially different.

Some recent studies performed the single cell electroporation. New electroporative methods bring about the ability to perform the single cell electroporation. For example, in the electroporative devices that used geometric variation to perform the electroporation, the width of the electroporative section could be adjusted to the diameter of each cell. Cells passing through the electroporative sections one by one can be electroporated individually. Trapping the single cells in individual positions also provides the ability of performing the single cell electroporation. Single cell electroporation have many advantages. It decreases the required applied voltage. The electroporation process can be monitored easily. It may allow a feedback control on the electroporation process of each cell, increase the cell viability and decrease the resealing times of the cell after electroporation.

7 Future trends

The rapid advancement in microfabrication techniques and in microfluidic control provides better opportunities for cell electroporation in microfluidic chips. Single cell electroporation can be performed. Cells can be monitored during electroporation. Higher viability and higher transfection rate of electroporation can be achieved. However, there are still some weak points associate with the current microfluidic electroporative devices that need further studies.

7.1 Cells

Most of the current studies work on the electroporation of cells in vitro. Cells usually attached to the supporting tissues that may have important effects on their functions. Besides, separating the cells from these attached tissues can damage the cell structure. Therefore, performing further comprehensive studies of the electroporation of cells in situ medium seems to be essential. This may result in the better understanding on the cell functionality. Although many studies work on the reversible electroporation of human cells, lack of any studies on the lysis of human cells is evident. Releasing the intercellular contents of these human cells can result in the better understanding on the cell structure and kinetic of the human cells. Some recent studies also focused on the electroporation of small cells such as *E. coli* cells. With the recent advancement in the micro (and even submicron)-manufacturing techniques more studies on these small cells can be expected in the future.

7.2 Lab-on-a-chip design

Lab-on-a-chip technology provides more possibility in researches related to life sciences. Feasibility of single cell study is one of the most important examples of Lab-on-a-chip technology (Gac et al. 2009; El-Ali et al. 2006). Among all the studies of the microfluidic electroporation devices, few of them tried to integrate the electroporation process with other post- and pre-processing such as cell detection, handling, and separation on a single lab-on-a-chip design. There are a few studies of the separation process after cell lysis (Sedgwick et al. 2008). Especially in the case of cell lysis, better methods and more advanced microchip designs are needed to separate released intercellular contents from the cell debris after the electroporation. Injecting the cells into the device is another issue that needs further attention. No devices have been reported to automatically select the cells and flow them through the electroporative sections. These steps usually are implemented manually which can damage the cell structure. Design and manufacturing of the fully automatic lab-on-a-chip devices that can perform all the pre- and post-processing in one single microchip (such as cell detection, handling, electroporative characteristics measurement, and separation) are highly desirable in the future. Detection of

the occurence and the measurement of the internalization during cell transfection also must be addressed in the future works. Up to know, the episode of cell internalization is predicted by eye. Although some studies put forward new methods to predict the cell electroporation, no method has been reported for predicting cell internalization yet. This is an important factor to design the completely automated cell transfection microfluidic devices.

7.3 Monitoring and control of electroporation process

It is important to monitor and control the effect of electric field on the cell membrane and structure during the electroporation. A few recent studies suggested innovative methods to predict the appearance of electropores on the cell membrane (Khine et al. 2005a, b). This method works on the basis of monitoring the electric field to predict the electroporation happening. Only one study conducted on the feedback control of electroporation in microfluidic device (Khine et al. 2007). The feedback control on the electroporation of single cells in microfluidic devices can prevent the excessive damage to the cell membrane structure, decrease the resealing time for the cell membrane after performing electroporation and increase the ability of one particular cell to be electroporated for many times.

By inventing new methods in the measurements of the cell membrane characteristics during the electroporation, further studies on the feedback control of the electroporation process should be performed. In these control systems, applied voltage can be controlled by monitoring and measurement of electrical parameters such as current and cell membrane resistance. Additionally, the pulse duration can be modified by using image processing methods. For example, the entrance of any colorful dyes into the cell can be recorded using image processing techniques. In this way, the minimum required applied voltage and pulse duration can be found to transfect the external molecules into the cell.

7.4 Theoretical studies

Analytical studies are essential to optimize, monitor, and control the performance of any microfluidic devices. There are many shortcomings associated with the electroporative devices that need further analytical studies. For example, there is not any theory that explains the exact mechanism behind the swelling of the cell in the applied electric field. Having the accurate theory to predict the kinetics of the electroporation can also allow us to design the control system which is not case-dependent.

The current analytical studies on cell electroporation have some underlying assumptions that must be considered carefully. First, cells are considered to be spherical. However, many previous studies show that the cells are elliptical and have a deformed shape under the applied electric field or pressure. Second, the cells are considered in an infinite domain. In reality, in microfluidic electroporation, cells are usually flow through the microchannels, the boundary effects on the electric field must be considered. Furthermore, the effect of cell expansion and rotation during the electroporation were not considered. More sophisticated models are needed to investigate the effects of electrodeformations such as swelling and rotation.

None of the current studies considered the effect of transmembrane potential on the transfection processes, i.e., the transport of ions, external molecules and nano-particles into the nanopores. Because of transmembrane potential, electroosmosis and electrophoresis effect must consider in the uptake rate of cells. Ionescu-Zanetti et al. (2008) showed that the electrophoresis effect could substantially improve the transfection efficiency in the cells. Therefore, having a comprehensive study on the effects of electrokinetic phenomena on the uptake rate of macromolecules and fluid flow is essential.

Effect of pulse shape on the electroporation efficiency can be important. Different pulse shapes can generate various effects on the cell (Fox et al. 2006). Some studies investigated the effect of different pulse shapes (Sinusoidal, step, and triangular) on the transmembrane potential and number of pores (Talele et al. 2010; Miklavcic and Towhidi 2010). Talele et al. (2010) developed a numerical model for a single cell electroporated by application of arbitrary external electric field pulses. They showed that pore density increases as long as a threshold V_m is maintained by the electric field. They also showed that the bipolar and short uni-polar pulses lead to the symmetrical and asymmetrical N (pore density) between the two polar regions of the cell, respectively. So far, no one has tried to optimize the pulse shape and duration to achieve the best results for the transmembrane potential, number of the pores, and pore area. One interesting method to find the optimize shape of the pulses is to use the "analogue to digital" technique to segment the general shape of the pulse and using genetic algorithm to find the optimum value for each section. In this method, the optimum value can be assigned to each discrete section and the pulse shape can be approximated by curve fitting of these discrete values.

Experimental studies showed that feedback control improves the electroporation efficiency of single cells (Cukjati et al. 2007; Khine et al. 2007). Feedback control can be utilized to monitor the radii of the pores and the time duration for which the pores remain open, and hence ensure the safe and accurate transfection during the reversible electroporation. Although a few experimental studies have been reported on the feedback control of the

single cell electroporation (Cukjati et al. 2007; Khine et al. 2007), more analytical studies for dynamic response of cell membrane to the external electric field must be performed to develop better feedback control of cell electroporation. Because of nonlinear behavior of the cell electroporation, many conventional controllers cannot be used. Other user-friendly control techniques (for example fuzzy logic) may be utilized to control the electroporation process.

8 Summary

In this article, the latest theoretical and experimental studies on microfluidics cell electroporation (or electropermeabilization) were reviewed. Based on the applications, microfluidic cell electroporation devices were categorized into three different groups. The advantages and disadvantages of the different methods in each group were compared with each other, particularly in terms of the transfection rate and the cell viability. Based on the status of the current studies, much more sophisticated theoretical studies on the cell membrane permeabilization and cell uptake process are needed. More studies on the feedback control during the cell electroporation and on the optimization of electric pulse shape should be conducted. Having the fully automated microfluidic cell electroporation devices integrated with pre- and post-processing steps are highly desirable.

Acknowledgments The authors wish to thank the financial support of the Canada Research Chair program and the Natural Sciences and Engineering Research Council (NSERC) of Canada through a research grant to D. Li.

References

Bao N, Wang J, Lu C (2008) Microfluidic electroporation for selective release of intracellular molecules at the single-cell level. Electrophoresis 29:2939–2944

Bao N, Le TT, Cheng J-X, Lu C (2010) Microfluidic electroporation of tumor and blood cells: observation of nucleus expansion and implications on selective analysis and purging of circulating tumor cells. Integr. Biol. 2:113–120. doi:10.1039/b919820b

Bilska AO, DeBruin KA, Krassowska W (2000) Theoretical modeling of the effects of shock duration, frequency, and strength on the degree of electroporation. Bioelectrochemistry 51:133–143

Brennan D et al (2009) Emerging optofluidic technologies for point-of-care genetic analysis systems: a review. Anal Bioanal Chem 395:621–636. doi:10.1007/s00216-009-2826-5

Brouzes E, Medkova M, Savenelli N, Marran D, Twardowski M, Hutchison JB, Rothberga JM, Linka DR, Perrimon N, Samuels ML (2009) Droplet microfluidic technology for single-cell high-throughput screening. PNAS 106(34):14195–14200

Cao Y, Yang J, Yin ZQ, Luo HY, Yang Mo, Hu N, Yang J, Huo DQ, Hou CJ, Jiang ZZ, Zhang RQ, Rong Xu, Zheng XL (2008) Study of high-throughput cell electrofusion in a microelectrode-array chip. Microfluid Nanofluid 5:669–675. doi:10.1007/s10404-008-0289-1

Cheng Wei et al (2010) Microfluidic cell arrays for metabolic monitoring of stimulated cardiomyocytes. Electrophoresis 31: 1405–1413

Cukjati D, Batiuskaite D, André F, Miklavčič D, Mir LM (2007) Mir real time electroporation control for accurate and safe in vivo non-viral gene therapy. Bioelectrochemistry 70:501–507

DeBruin KA, Krassowska W (1999a) Modeling electroporation in a single cell. I. Effects of field strength and rest potential. Biophys J 77:1213–1224

DeBruin KA, Krassowska W (1999b) Modeling electroporation in a single cell. ii. Effects of ionic concentrations. Biophys J 77: 1225–1233

El-Ali J, Sorger PK, Jensen KF (2006) Cells on chips. Nature. 442:403–411. doi:10.1038/nature05063

Escoffre JM, Portet T, Wasungu L, Teissié J, Dean D, Rols MP (2009) What is (Still not) known of the mechanism by which electroporation mediates gene transfer and expression in cells and tissues. Mol Biotechnol 41:286–295

Fei Z et al (2007) Gene transfection of mammalian cells using membrane sandwich electroporation. Anal. Chem. 79(15):5719–5722

Fei Z et al (2010) Micronozzle Array enhanced sandwich electroporation of embryonic stem cells. Anal Chem 82:353–358

Fox MB, Esveld DC, Valero A, Luttge R, Mastwijk HC, Bartels PV, van den Berg A, Boom RM (2006) Electroporation of cells in microfluidic devices: a review. Anal Bioanal Chem 385:474–485

Fox MB et al (2008) Inactivation of *L.* plantarum in a PEF microreactor the effect of pulse width and temperature on the inactivation. Innovative Food Science and Emerging Technologies. 9:101–108

Geng T et al (2010) Flow-through electroporation based on constant voltage for large-volume transfection of cells. J Controlled Release. doi:10.1016/j.jconrel.2010.01.030

Gimsa Jan (2001) A comprehensive approach to electro-orientation, electrodeformation, dielectrophoresis, and electrorotation of ellipsoidal particles and biological cells. Bioelectrochemistry 54:23–31

Granot Y, Rubinsky B (2008) Mass transfer model for drug delivery in tissue cells with reversible electroporation. Int J Heat Mass Transfr 51:5610–5616

Ho Yi-P, Leong KM (2010) Quantum dot-based theranostics. Nanoscale 2:60–68

Huang Y, Rubinsky B (2000) Micro-electroporation: improving the efficiency and understanding of electrical permeabilization of cells. Biomed Microdev 3:145–150

Huang Y, Rubinsky B (2001) Microfabricated electroporation chip for single cell membrane permeabilization. Sens Actuators A 89:242–249

Huang Y, Rubinsky B (2003) Flow-through micro-electroporation chip for high efficiency single-cell genetic manipulation. Sens Actuators A 104:205–212

Ikeda N, Tanaka N, Yanagida Y, Hatsuzawa T (2007) On-chip single-cell lysis for extracting intracellular material. Jpn J Appl Phys 46(9B):6410–6414

Ionescu-Zanetti C, Blatz A, Khine M (2008) Electrophoresis-assisted single-cell electroporation for efficient intracellular delivery. Biomed Microdevices 10:113–116. doi:10.1007/s10544-007-9115-x

Kang Y, Li D, Kalams SA, Eid JE (2008) DC-dielectrophoretic separation of biological cells by size. Biomedical Microdevices 10(2):243–249

Khine M, Lau A, Ionescu-Zanetti C, Seo J, Lee LP (2005) A single cell electroporation chip. Lab Chip 5:38–43. doi:10.1039/b408352k

Khine M, Ionescu-Zanetti C, Blatz A, Wang L-P, Lee LP (2007) Single-cell electroporation arrays with real-time monitoring and feedback control. Lab Chip 7:457–462

Kim SK, Kim JH, Kim KP, Chung TK (2007) Continuous low-voltage dc electroporation on a microfluidic chip with polyelectrolytic salt bridges. Anal. Chem. 79:7761–7766

Krassowska W, Filev PD (2007) Modeling electroporation in a single cell. Biophys J 92:404–417

Le Gac S, van den Berg A (2009) Single cells as experimentation units in lab-on-a-chip devices. Trends Biotechnol 28(1). doi: 10.1016/j.tibtech.2009.10.005

Lee S-W, Tai Y-C (1999) A micro cell lysis device. Sens Actuators A 73:74–79

Lee ES, Robinson D, Rognlien JL, Harnett CK, Simmons BA, Bowe Ellis CR, Davalos RV (2006) Microfluidic electroporation of robust 10-μm vesicles for manipulation of picoliter volumes. Bioelectrochemistry 69:117–125

Lee WG, Demirci U, Khademhosseini A (2009) Microscale electroporation: challenges and perspectives for clinical applications. Integrative Biology. 1:242–251

Li D (2004) Electrokinetics in microfluidics. Elsevier, Amsterdam

Li D (2008a) Encyclopedia of microfluidics and nanofluidics. Springer, New York

Li S (2008b) Electroporation protocols: preclinical and clinical gene medicine. Springer, New York

Lim JK, Zhou H, Tilton RD (2009) Liposome rupture and contents release over coplanar microelectrode arrays. J Colloid Interf Sci 332:113–121

Lin Y-H, Leea G-B (2009) An optically induced cell lysis device using dielectrophoresis. Appl Phys Lett 94:033901

Lu H, Schmidt MA, Jensen KF (2005) A microfluidic electroporation device for cell lysis. Lab on a Chip 5:23–29

Luo C, Yang X, Fu Q, Sun M, Ouyang Q, Chen Y, Ji H (2006) Picoliter-volume aqueous droplets in oil: Electrochemical detection and yeast cell electroporation. Electrophoresis 27:1977–1983

Miklavcic D, Towhidi L (2010) Numerical study of the electroporation pulse shape effect on molecular uptake of biological cells. Radiol Oncol. 44(1):34–41

Mossop BJ, Barr RC, Henshaw JW, Yuan F (2007) Electric fields around and within single cells during electroporation—a model study. Ann Biomed Eng. 35(7):1264–1275

Neu JC, Krassowska W (1999) Asymptotic model of electroporation. Phys Rev E 59:3471–3482

Neu WK, Neu JC (2009) Theory of electroporation. In: Efimov IR, Kroll MW, Tchou PJ (eds) Cardiac bioelectric therapy. Springer, New York

Neumann E, Schaefer-Ridder M, Wang Y, Hofschneider PH (1982) Gene transfer into mouse lyoma cells by electroporation in high electric fields. EMBO J 1:841–845

Park S, Chung TK, Kim HC (2009) Ion bridges in microfluidic systems. Microfluid Nanofluid 6:315–331. doi:10.1007/s10404-008-0391-4

Schaper J, Bohnenkamp HR, Noll T (2007) New electrofusion devices for the improved generation of dendritic cell-tumour cell hybrids. In: Smith R (ed) Cell technology for cell products. Springer, New York

Sedgwick H, Caron F, Monaghan PB, Kolch W, Cooper JM (2008) Lab-on-a-chip technologies for proteomic analysis from isolated cells. J. R. Soc Interface 5:S123–S130

Shil P, Bidaye S, Vidyasagar PB (2008) Analysing the effects of surface distribution of pores in cell electroporation for a cell membrane containing cholesterol. J Phys D 41:055502 (7 pp)

Shin YS, Cho K, Kim JK, Lim SH, Park CH, Lee KB, Park Y, Chung C, Han D-C, Chang JK (2004) Electrotransfection of mammalian cells using microchannel-type electroporation chip. Anal Chem 76:7045–7052

Sott K et al (2008) Optical systems for single cell study. Expert Opin Drug Discov 3(11)

Suzuki T, Yamamoto H, Ohoka M, Okonogi A, Kabata H, Kanno I, Washizu M, Kotera H (2007) High throughput cell electroporation array fabricated by single-mask inclined uv lithography exposure and oxygen plasma etching. In: The 14th international conference on solid-state sensors, actuators and microsystems, June 10–14, 2007. IEEE, Lyon, pp 687–690

Talele S, Gaynor P, Cree MJ, van Ekeran J (2010) Modelling single cell electroporation with bipolar pulse parameters and dynamic pore radii. J Electrostat 1–14

Teissie J, Eynard N, Vernhes MC, Be′nichou A, Ganeva V, Galutzov B, Cabanes PA (2002) Recent biotechnological developments of electropulsation. A prospective review. Bioelectrochemistry 55:107–112

Teissie J, Golzio M, Rols MP (2005) Mechanisms of cell membrane electropermeabilization: A minireview of our present (lack of ?) knowledge. Biochim Biophys Acta 1724:270–280

Valero A, Post JN, van Nieuwkasteele JW, ter Braak PM, Kruijer W, van den Berg A (2008) Gene transfer and protein dynamics in stem cells using single cell electroporation in a microfluidic device. Lab Chip 8:62–67. doi:10.1039/b713420g

Valley JK, Hsu H-Y, Neale S, Ohta AT, Jamshidi A, Wu MC (2009a) Assessment of single cell viability following light induced electroporation through use of on-chip microfluidics IEEE. 978-1-4244-2978-3

Valley JK, Neale S, Hsu H-Y, Ohta AT, Jamshidi A, Wu MC (2009b) Parallel single-cell light-induced electroporation and dielectrophoretic manipulation. Lab on a Chip 9:1714–1720. doi: 10.1039/b821678a

Vassanelli S, Bandiera L, Borgo M, Cellere G, Santoni L, Bersani C, Salamon M, Zaccolo M, Lorenzelli L, Girardi S, Maschietto M, Dal Maschio M, Paccagnella A (2008) Space and time-resolved gene expression experiments on cultured mammalian cells by a single-cell electroporation microarray. New Biotechnol 25(1). doi:10.1016/j.nbt.2008.03.002

Wang H-Y, Lu C (2006a) Electroporation of mammalian cells in a microfluidic channel with geometric variation. Anal Chem. 78:5158–5164

Wang H-Y, Lu V (2006b) High-throughput and real-time study of single cell electroporation using microfluidics: effects of medium osmolarity. Biotechnology and Bioengineering 95(6): 1116–1125. doi:10.1002/bit

Wang H-Y, Lu C (2008) Microfluidic electroporation for delivery of small molecules and genes into cells using a common dc power supply. Biotechnology and Bioengineering 100(3):579–586. doi: 10.1002/bit.21784

Wang H-Y, Bhunia AK, Lu C (2006) A microfluidic flow-through device for high throughput electrical lysis of bacterial cells based on continuous dc voltage. Biosens Bioelectronics 22:582–588

Wang J, Stine MJ, Lu C (2007) Microfluidic cell electroporation using a mechanical valve. Anal Chem 79:9584–9587

Wang J, Bao N, Paris LL, Wang H-Y, Geahlen RL, Lu C (2008) Detection of kinase translocation using microfluidic electroporative flow cytometry. Anal Chem 80(4):1087–1093

Wang M et al (2010) Single-cell electroporation. Anal Bioanal Chem. 397:3235–3248

Weaver JC, Chizmadzhev YuA (1996) Theory of electroporation: a review. Bioelectrochem Bioenerg 41:135–160

Zaharoff DA, Henshaw JW, Mossop B, Yuan F (2008) Mechanistic analysis of electroporation-induced cellular uptake of macromolecules. 94–105. doi:10.3181/0704-RM-113

Zhan Y, Wang J, Bao N, Lu C (2009) Electroporation of cells in microfluidic droplets. Anal Chem 81:2027–2031. doi:10.1021/ac9001172

Zhao X, Zhang M, Yang R (2010) Control of pore radius regulation for electroporation-based drug delivery. Commun Nonlinear Sci Numer Simul 15:1400–1407

Zhu T et al (2010) Electroporation based on hydrodynamic focusing of microfluidics with low dc voltage. Biomed Microdevices 12:35–40. doi:10.1007/s10544-009-9355-z

Ziaie B et al (2004) Hard and soft micromachining for BioMEMS: review of techniques and examples of applications in microfluidics and drug delivery. Advanced Drug Delivery Reviews. 56(3):145–172